Lithospheric Layering in the North American Craton

Huaiyu Yuan *(Berkeley Seismological Laboratory),* **Barbara Romanowicz** *(Berkeley Seismological Laboratory)*

Recent receiver function studies detect structural boundaries under continental cratons at depths too shallow to be consistent with the lithosphere-asthenosphere boundary (LAB) as inferred from seismic tomography and other geophysical studies. Using the new results from our regional surface wave tomographic inversion for the North American upper mantle shear wave structure, we show (Figure1) that changes in the direction of azimuthal anisotropy with depth reveal the presence of two distinct lithospheric layers throughout the stable part of the North American (NA) continent [*Yuan and Romanowicz*, 2010]. (Figure 1 here) The top layer is thick (~150 km) under the Archean core and tapers out on the Paleozoic borders. Its thickness variations follow those of a highly depleted layer inferred from thermo-barometric analysis of xenoliths [*Griffin et al.*, 2004]. The LAB is relatively flat (180-240km), in agreement with the presence of a thermal conductive root that subsequently formed around the depleted chemical layer [*Cooper et al.*, 2004]. Our findings tie together seismological, geochemical and geodynamical studies of the cratonic lithosphere in North America. They also suggest that the horizon detected in receiver function studies likely corresponds to the sharp mid-lithospheric boundary rather than to the more gradual LAB. The change of fast axis direction of azimuthal anisotropy with depth is a powerful tool for the detection of lithospheric layering under continents. Our study indicates that the "tectosphere" is no thicker than ~200-240km and that its chemically most depleted part reaches thicknesses of ~160-170 km (Figure 1). While the morphology of the North American craton may be exceptionally simple, the application of this tool to other continents should provide further insights on the assembly and evolution of cratons worldwide.

References

Cooper, C. M., A. Lenardic, and L. Moresi (2004), The thermal structure of stable continental lithosphere within a dynamic mantle, *Earth Planet. Sci. Lett., 222*(3-4), 807-817.

Griffin, W. L., S. Y. O'Reilly, B. J. Doyle, N. J. Pearson, H. Coopersmith, K. Kivi, V. Malkovets, and N. Pokhilenko (2004), Lithosphere mapping beneath the North American plate, *Lithos, 77*(1-4), 873-922.

Yuan, H., and B. Romanowicz (2010), Lithospheric layering in the North American Craton, *Nature*, DOI: 10.1038/nature09332, in press.

Acknowledgements: This study was supported by NSF EAR-0643060 grant to BR. We are grateful to the IRIS DMC and the Geological Survey of Canada for providing the waveforms, K. Liu, M. Fouch, R. Allen, A. Frederiksen and A. Courtier for sharing their SKS splitting measurements, and S. Whitmeyer and K. Karlstrom for providing their Proterozoic Laurentia structural map.

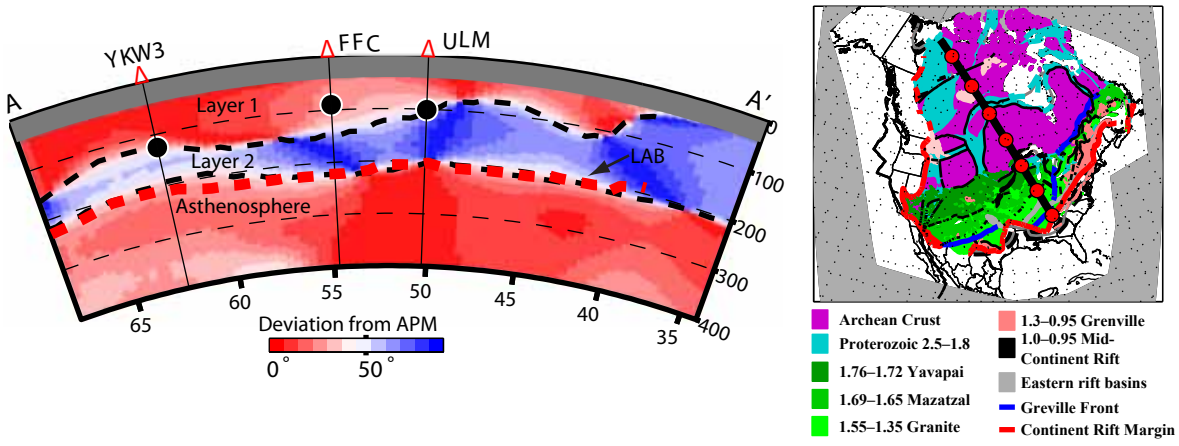

Upper mantle layering defined by changes in the direction of fast axis of azimuthal anisotropy. Left: deviation of the fast axis direction from the NA absolute plate motion direction, as a function of depth along a depth cross-section AA. Rapid changes of the fast axis directions mark the boundarie

Survival and Demise of Thick Continental Lithosphere under Highly Extended Crust

Vera Schulte-Pelkum *(University of Colorado at Boulder),* **Glenn Biasi** *(University of Nevada, Reno),* **Anne Sheehan** *(University of Colorado at Boulder),* **Craig Jones** *(University of Colorado at Boulder)*

We find an unusually thick lithosphere under a highly extended portion of the Basin and Range. We determined Moho depths using P-to-S receiver functions from the EarthScope Transportable Array and the Southern Great Basin Digital Seismic Network. As one would expect from isostasy, the crust is thicker under the high-elevation Northern Basin and Range and thinner in the low-lying Southern Basin and Range. However, we find an unexpected crustal keel under the highly extended Death Valley extensional area in between, underlying low surface elevations and putting the crust well outside of isostatic equilibrium. Dense crust is not found in this area in refraction results, but a lithospheric mantle keel fits the seismic observations as well as the observation of anomalous isotope ratios in basalts from this area that require an old, enriched lithospheric source [*Farmer et al., 1989*]. Unusually low εNd values indicating an old lithospheric mantle source were replaced by asthenospheric basalts in the Lake Mead extensional area, but persist during the entire history of basaltic magmatism (12-0 Ma) in the Death Valley extensional area, matching the geographical extent of dense mantle. If the anomaly is isostatic and a lithosphere-asthenosphere density contrast of 50 kg/m^3 (0.05 g/cm^3) is assumed, the lithosphere-asthenosphere boundary lies at a mean depth of 120 km within the anomaly, compared to a mean of 40 km outside the anomaly. We conclude that deformation was highly incoherent between the surface and the lower crust and mantle lithosphere, and that an island of Precambrian lithosphere has survived beneath the Death Valley extensional area and may currently be sinking.

References

Farmer, G.L., F.V. Perry, S. Semken, B. Crowe, D. Curtis, D.J. DePaolo, Isotopic evidence on the structure and origin of subcontinental lithospheric mantle in southern Nevada, *J. Geophys. Res. 94*, B6, 7885-7898, 1989

Acknowledgements: This research is funded by NSF grant EAR-0838509. Seismic data with the exception of those from the Southern Great Basin Digital Seismic Network were obtained from the IRIS DMC.

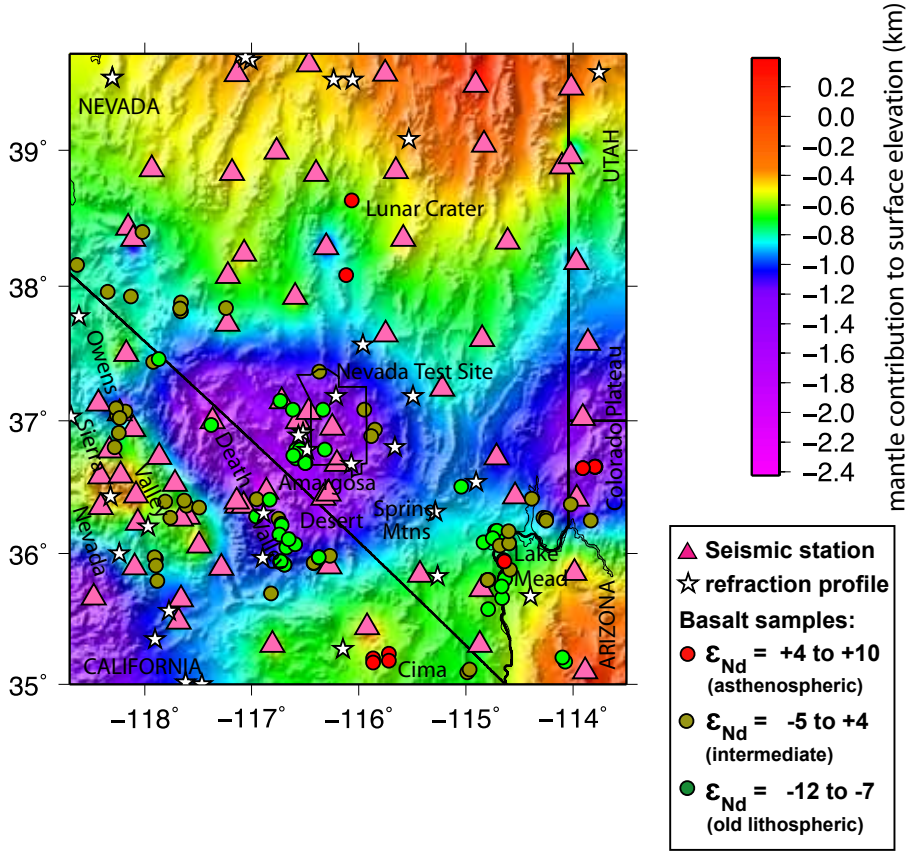

Mantle contribution to surface elevation (color), overlaid by topography (shading) for orientation. Pink triangles (seismic stations) are location where Moho depth was measured, white stars (refraction profile centers) mark crustal velocity and density values from refraction experiments used to convert receiver function Moho times to depth and to calculate isostatic contribution of the crust. Mantle buoyancy is well constrained in areas where both seismic stations and refraction data exist in the vicinity. Circles mark locations of basalts with measured Neodymium isotope ratios and are plotted so that younger samples overlay older ones.

The Lithospheric Structure of the Mendocino Triple Junction from Receiver Function Analysis

Yongbo Zhai *(Rice University),* **Alan Levander** *(Rice University)*

The Mendocino Triple Junction (MTJ), which occurs offshore from Cape Mendocino at ~ 40.50N in northern California, is the intersection of the Gorda plate, Pacific plate, and North American plate. It was formed ~28 Ma when the Pacific spreading ridge first contacted the western margin of the North American plate. In rigid plate frame, the northward migrating MTJ leaves in its wake a slab-free region filled by upwelling asthenospheric mantle just south of the Gorda plate, widely known as the "slab window" model.

To examine the lithospheric structure in the MTJ region, especially the structure of the "slab window", we generated a 3D PdS receiver function CCP image. We used 186 earthquakes recorded at 111 broadband stations of the Flexible Array Mendocino Experiment (FAME) together with the Berkeley Digital Seismic Network and USArray Transportable Array. The data were depth mapped and laterally migrated incorporating 3D traveltime corrections determined from 3D P-and S-tomography models.

The resulting image confirms the crustal structure of the Mendocino Triple Junction Seismic Experiment (MTJSE) and reveals detailed lithospheric structure. The top and bottom of the Gorda slab are identified by the Moho and Lithosphere-Asthenosphere Boundary (LAB) in the subduction regime, showing that the thickness of the Gorda slab is ~ 40 km, comparable with that predicted by half-space cooling model. The "slab window" in the transform regime has a complex structure, but its top can be traced continuously to the Gorda LAB, although the transition is more abrupt than that suggested by the refraction velocity model. The LAB is shallowest beneath Clear Lake volcano and Lake Pillsbury where high heat flow and basalt intrusions are observed respectively. Under the western part of northern Great Valley, the Moho signal is absent, likely due to the hydration and serpentinization of the upper mantle during the subduction of the Gorda slab ~2Ma. The Great Valley ophiolite is observed at the crustal depth instead.

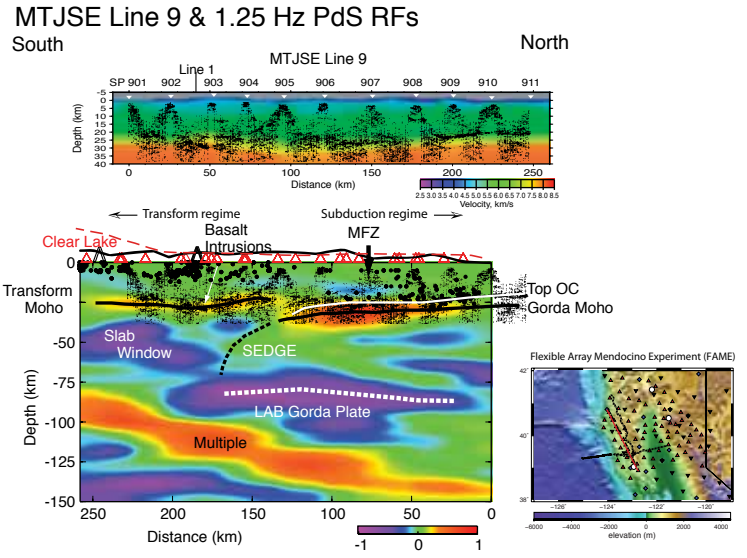

Figure 1. Coast-range-parallel receiver function cross-section. P-wave velocity model of MTJSE line 9 is shown in the upper panel, superimposed by the depth migrated single-fold section. The black solid line on top of the CCP image schematically shows the surface elevation along the cross-section, whereas the red dashed line schematically shows the heat flow. The red triangles denote projected stations, and the black dots denote the projected earthquake hypocenters since 1985 with M > 3.0. The three strong events in the CCP image in order of depth are the Moho, LAB, and first Moho multiple respectively. The black lines mark the Moho depth determined by the RF image, and white lines mark the top and bottom of the Gorda slab. The basalt intrusions near Lake Pillsbury are represented by strong reflections of the depth migrated section from the lower crust and Moho. Black dashed line illustrates the southern edge of the Gorda plate, which dips to the south.

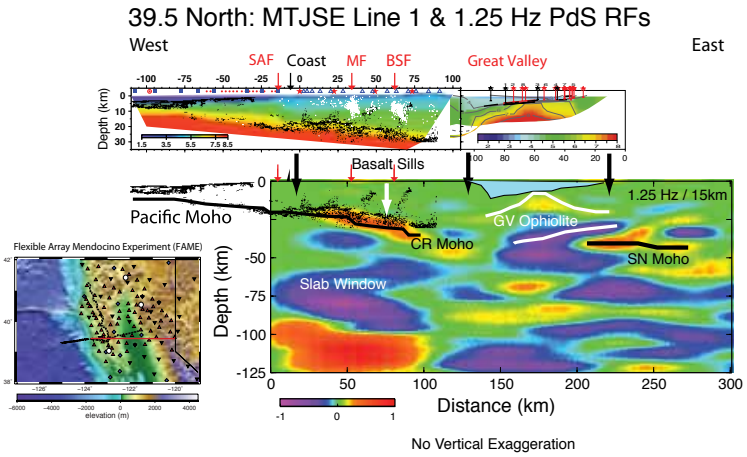

Figure 2. East-west receiver function cross-section at 39.50N. P-wave velocity model of the MTJSE line 1 is shown in the upper panel, superimposed by the depth migrated single-fold section. The white dots denote the projected earthquakes beneath the Maacama Fault and Bartlett Springs Fault. The black lines mark the Moho depth determined by the RF image. The basalt intrusions near Lake Pillsbury are represented by strong reflections from the lower crust and Moho. The Great Valley Ophiolite (GVO) is a high velocity body bounded by white lines between the Coast Ranges (CR) and Sierra Nevada (SN) Moho. Note that no clear Moho signal is observed beneath the northern Great Valley.

References

Zhai, Y., and A. Levander (2010), The Lithosphere-Asthenosphere Boundary and the Slab Window in the Mendocino Triple Junction Region, in preparation.

Acknowledgements: This project is supported by NSF grants EAR-0642474 and EAR-0746379.

Lithospheric Structure beneath the Western US Using USArray Data

Meghan S. Miller *(University of Southern California),* **Alan Levander** *(Rice University)*

Using a combination teleseismic data from the USArray Transportable Array, previous PASSCAL experiments, and the COARSE array in Arizona we have produced images of the lithospheric structure beneath the Western United States. We have made common conversion point (CCP) stacked Ps and Sp receiver function image volumes to determine, in more detail and higher resolution than previously obtained, the crustal thickness and the depth to the Moho and lithosphere-asthenosphere boundary (LAB) throughout the Western U.S. Individual receiver functions have been converted to depth and laterally "migrated" to their conversion point using 3D P- and S-wave tomography velocity models, with redundant signals stacked for signal enhancement. Both S and P receiver functions have imaged an unusually complex crust-mantle boundary region beneath the Colorado Plateau in comparison to most other parts of the western U.S., although we also see features that correlate with expressions of lithospheric drips in the southern Sierra Nevada and the Wallowa Mountains. The Moho shallows significantly from an average of ≥40 km to the southern Basin and Range, where the crust is ~30 km. These complications in the Moho are correlated with low upper mantle velocities observed in P and S body wave tomography and S-velocity structure determined from Rayleigh wave inversion. Throughout the model, the LAB is a negative amplitude feature that has significant topographic variation, and cannot be described as a single surface. We see a particularly strong correlation between calculated equilibration pressures of primitive basalt whole rock samples from across the western United States, extracted from the NAVDAT database (http://www.navdat.org/), and the LAB estimate from the Sp images beneath the southern Basin and Range, the Colorado Plateau, and the Sierra Nevada. The depth estimates from the geochemistry data and comparison with the PdS receiver function images for the same region allows us to interpret the lithosphere-asthenosphere boundary and its relation to the tectonic provinces in the western United States. We will present different geologic scenarios that can explain these structures.

Acknowledgements: We would like to thank Kaijian Liu, Yongbo Zhai, Yan Xu, and Meijuan Jiang for assisting with data processing. The Sp receiver function study began as an exercise at the 2008 CIDER (Cooperative Institute for Deep Earth Research) summer school. This research was funded by Earthscope grant EAR-0844741 and 0844760. AL gratefully acknowledges a Humboldt Research Prize from the Alexander von Humboldt Foundation. The Ps study was initiated by AL while on sabbatical at the GeoForschungsZentrum Potsdam, Germany.

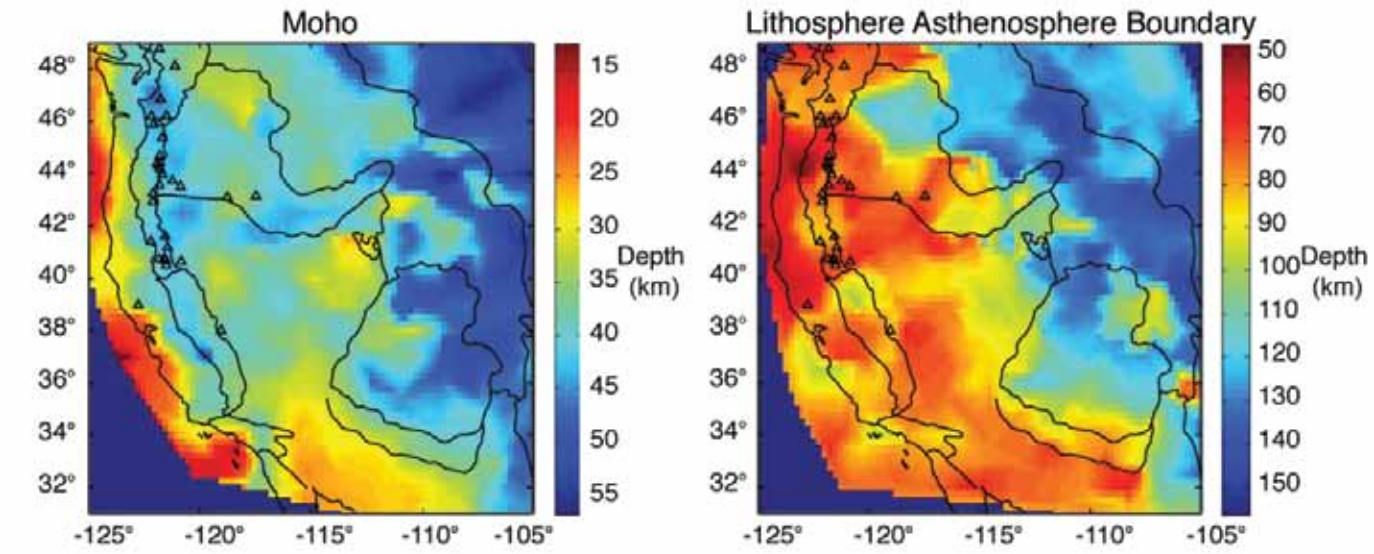

Maps of depth to (a) Moho and (b) LAB. The thick lines illustrate the physiographic boundaries in the western U.S. The LAB map is a smoothed estimate of the shallowest event we identified as the LAB in the Ps and Sp receiver functions.

The Lithosphere-Asthenosphere Boundary beneath North America and Australia

Heather A. Ford *(Brown University),* **David L. Abt** *(ExxonMobil Exploration Company),* **Karen M. Fischer** *(Brown University)*

The concept of a strong lithosphere that translates as a relatively coherent layer over a weak asthenosphere is fundamental to models of plate motions, tectonics, and mantle convection. However, much remains to be learned about the physical and chemical properties that create rheological differences between the lithosphere and asthenosphere. We have used Sp and Ps scattered waves to image mantle discontinuities beneath North America and Australia.

In the tectonically active western U.S., large portions of the Phanerozoic eastern U.S., Phanerozoic eastern Australia and the adjacent edge of the Australian craton, prominent Sp phases from a negative velocity contrast were found at depths of 50-130 km, consistent with the lithosphere-asthenosphere boundary depth range from surface wave tomography. These phases imply significant (4-10%) velocity drops over depth ranges of 30-40 km or less, and thus cannot be simply explained by a lithosphere-asthenosphere boundary that is governed purely by temperature. Rather, they imply that the asthenosphere is hydrated with respect to a drier, depleted lithosphere or contains a small amount of partial melt.

In contrast, no significant negative Sp phase was found at the base of the thick cratonic lithosphere in either continent, implying that the cratonic lithosphere-asthenosphere velocity gradient is distributed over more than 50-70 km in depth. This gradient may be purely thermal in origin, although gradational changes in composition or melt content cannot be ruled out. A negative discontinuity internal to the cratonic lithosphere was observed at depths of 50-115 km. The depth of this boundary is comparable to the thickness of oceanic and younger continental lithosphere. This discontinuity may date from the formation of the cratonic lithosphere, or it could reflect later alteration of the cratonic lithosphere by melting and metasomatism, perhaps as the top of a melt cumulate layer.

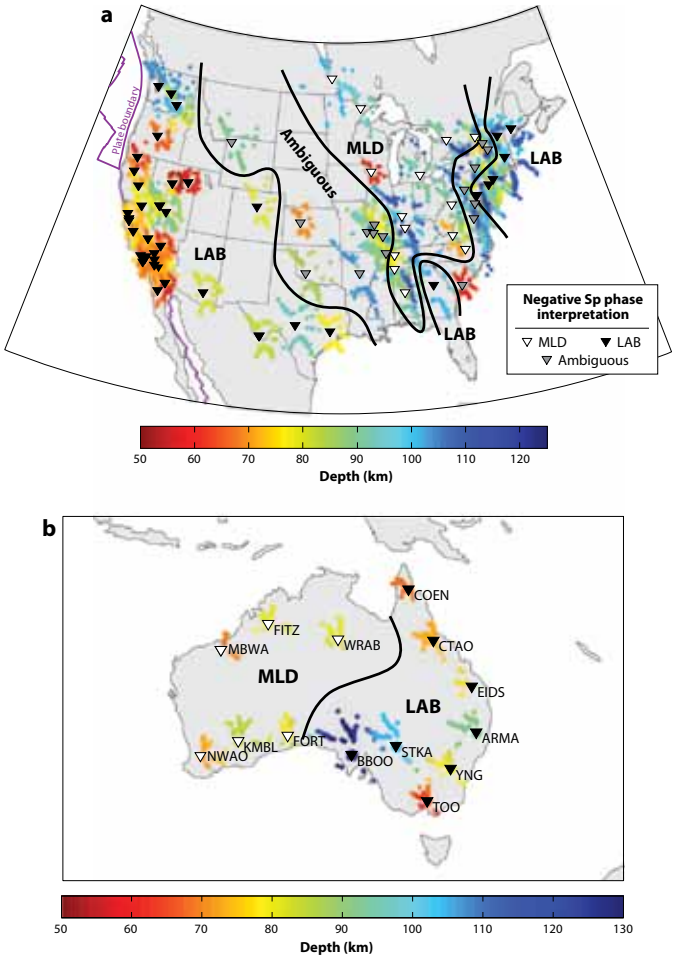

Mantle discontinuity depths estimated from Sp receiver functions in North America by Abt et al. (2010) (a) and in Australia by Ford et al. (2010) (b). The dots are colored for depth/amplitude and represent Sp piercing points that have been interpolated onto a fine grid and smoothed with a circular filter with a 30 km radius. (a) North America. Black inverted triangles indicate stations where the negative Sp phase is interpreted as the lithosphere-asthenosphere boundary (LAB), white inverted triangles are stations where the phase is interpreted as a mid-lithospheric discontinuity (MLD), and gray stations indicate ambiguity in the interpretation of the negative Sp phase. (b) Australia. Negative Sp phases at stations in Phanerozoic eastern Australia and just within the eastern margin of the Proterozoic craton (BBOO and stations to its east) are interpreted as the LAB. Negative Sp phases at most stations in the Proterozoic and Archean craton (station WRAB and the stations to its west

References

Ford, H. A., K. M. Fischer, D. L. Abt, Catherine A. Rychert, L. T. Elkins-Tanton (2010), The lithosphere-asthenosphere boundary and cratonic lithospheric layering beneath Australia from Sp wave imaging, *Earth Planet. Sci. Lett.*, submitted.

Abt, D. L., K. M. Fischer, S.W. French, H.A. Ford, H. Yuan, B. Romanowicz (2010), North American lithospheric discontinuity structure imaged by Ps and Sp receiver functions, *J. Geophys. Res.*, in press.

Fischer, K. M., H. A. Ford, D. L. Abt, C. A. Rychert (2010), The lithosphere-asthenosphere boundary, *Ann. Rev. Earth Planet. Sci., 38*, 551-575.

Acknowledgements: Data used in these studies were collected from the IRIS DMS. This work was supported by the National Science Foundation under awards EAR-0538155 (Geophysics) and EAR-0641772 (EarthScope).

Receiver Function Imaging of the Lithosphere-Asthenosphere Boundary

Catherine A. Rychert *(University of Bristol, U.K.),* **Peter M. Shearer** *(University of California, San Diego, U.S.A.)*

The lithosphere-asthenosphere boundary, or LAB, is often defined seismically as the top of the low velocity zone underlying the higher velocities of the lithospheric lid. Surface-wave studies have shown the global extent of upper-mantle low-velocity zones, but do not have the vertical resolution to constrain the details of LAB depth and sharpness. Better depth resolution, at least in the vicinity of seismic stations, is provided by receiver-function studies of converted phases, although care must be taken to distinguish LAB signals from noise and crustal reverberations. The continued operation of the global seismic networks, by IRIS and other agencies, has provided a sufficient volume of data that receiver-function imaging of the LAB is now possible on a global scale. We have analyzed 15 years of global seismic data using P-to-S (Ps) converted phases from over 150 stations and imaged an interface that correlates with tectonic environment, varying in average depth from 95 ± 4 km beneath Precambrian shields and platforms to 81 ± 2 km beneath tectonically altered regions and 70 ± 4 km at oceanic island stations. Because the polarity of the Ps arrivals indicates a shear-velocity drop with depth, this interface is likely the LAB in most regions, although it may constitute another boundary beneath the cratonic interiors of continents where the LAB is expected to be much deeper. The high frequencies observed in the Ps arrivals require a sharp discontinuity, implying a change in composition, melting, or anisotropy, not temperature alone.

References

Rychert, C. A., and P. M. Shearer, A global view of the lithosphere-asthenosphere boundary, *Science, 324*, 2009.

Rychert, C. A., P. M. Shearer and K. M. Fischer, Scattered wave imaging of the lithosphere-asthenosphere boundary, *Lithos, 2010*.

Jordan, T. H., Global Tectonic regionalization for seismological data analysis, *Bull. Seismol. Soc. Amer., 71*(4): 1131-1141, 1981.

Acknowledgements: This research was supported by National Science Foundation awards EAR-0229323 and EAR-0710881.

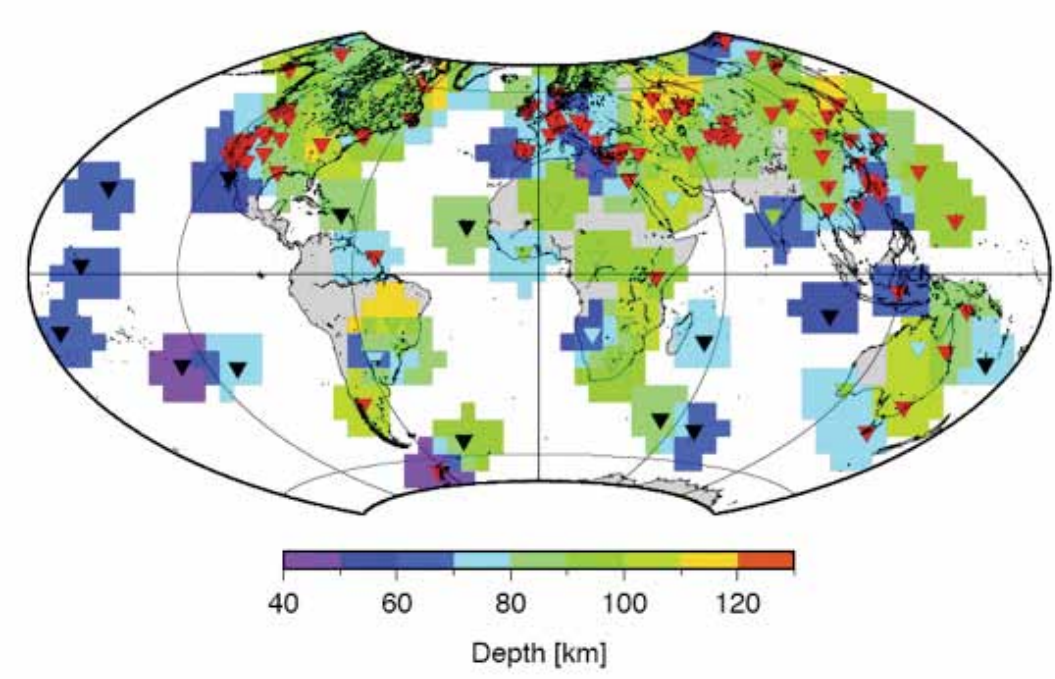

Global map of the depth to the lithosphere-asthenosphere boundary imaged using Ps receiver functions. Color indicates depth. Triangles show the 169 stations used in this study. Station color corresponds to tectonic regionalization, after Jordan (1981). Tectonic regions colored as follows: Oceanic – black, Phanerozoic orogenic zones and magmatic belts – red, Phanerozoic platforms – cyan, Precambrian shields and platforms – green. Although the work of Jordan (1981) divides oceanic environments into three age groupings, a single oceanic bin, encompassing all ages, is used here, since sampling of this region is sparse.

S-Velocity Structure of Cratons, from Broad-Band Surface-Wave Dispersion

Sergei Lebedev *(Dublin Institute for Advanced Studies),* **Jeannot Trampert** *(Utrecht University)*

Despite recent progress in mapping the lateral extent of cratonic roots worldwide [e.g. Lebedev & van der Hilst, 2008], profiles of seismic velocities within them remain uncertain. Here, a novel combination of waveform-analysis techniques was used to measure inter-station, Rayleigh- and Love-wave phase velocities in broad period ranges. The new measurements yield resolution from the upper crust to deep upper mantle beneath a selection of cratons from around the globe and provide new constraints on the thermal and compositional structure and evolution of Precambrian lithosphere.

Shear-wave speed Vs is consistently higher in the lithosphere of cratons than in the lithosphere of Proterozoic foldbelts. Because known effects of compositional variations in the lithosphere on Vs are too small to account for the difference, this confirms that temperature in the cratonic lithosphere is consistently lower. This is in spite of sub-lithospheric mantle beneath continents being thermally heterogeneous, with some cratons currently underlain by a substantially hotter asthenosphere compared to others.

An increase in Vs between the Moho and a 100-150 km depth is consistently preferred by the data and is likely to be due to phase transformations, in particular the transition from spinel peridotite to garnet peridotite, proposed previously to give rise to the "Hales discontinuity" within this depth interval. The depth and the width of the phase transformation depend on mantle composition; it is likely to occur deeper and over a broader depth interval beneath cratons than elsewhere because of the high Cr content in the depleted cratonic lithosphere, as evidenced by a number of xenolith studies. Seismic data available at present would be consistent with both a sharp and a gradual increase in Vs in the upper lithosphere (a Hales discontinuity or a "Hales gradient").

Radial anisotropy in the upper crust indicates vertically oriented anisotropic fabric (Vsh < Vsv); this may yield a clue on how cratons grew, lending support to the view that distributed crustal shortening with sub-vertical flow patterns occurred over large scales in hot ancient orogens. In the lower crust and upper lithospheric mantle, radial anisotropy reveals horizontal fabric (Vsh > Vsv), likely to be a record of horizontal ductile flow in the lower crust and lithospheric mantle at the time of the formation and stabilisation of the cratons.

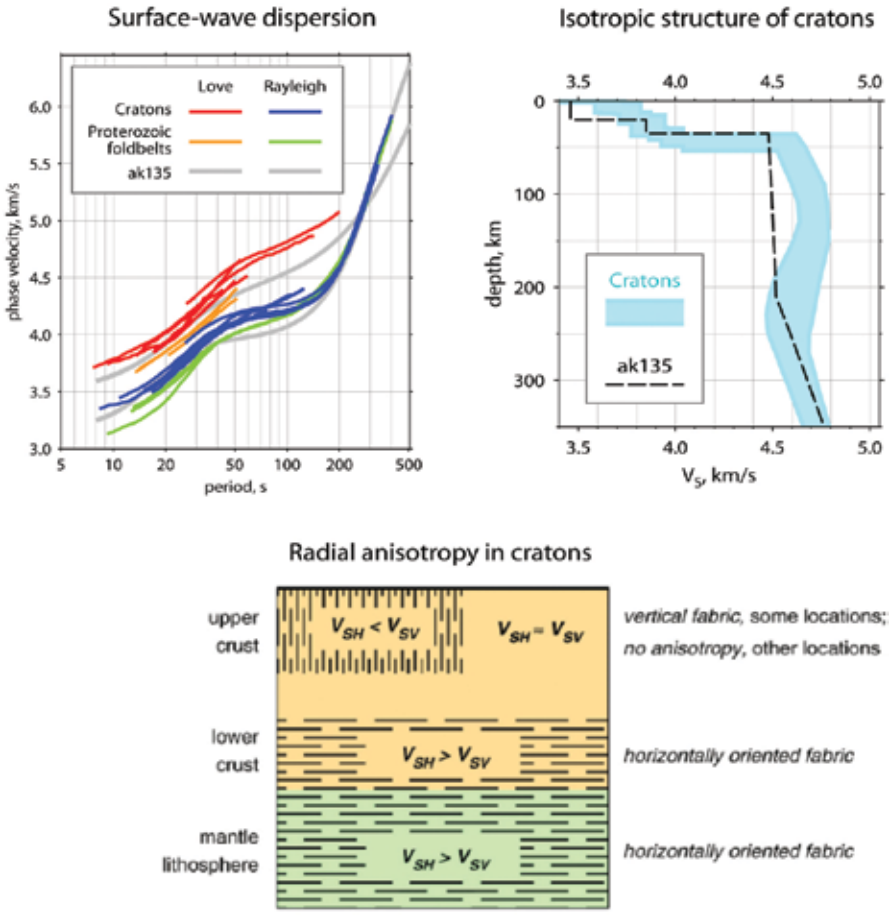

Top left: phase-velocity measurements sampling Precambrian continental lithosphere. Top right: summary profile of the isotropic-average shear speed beneath Archean cratons. The ranges of Vs values include the best-fitting profiles from all the cratonic locations sampled. Bottom: radial anisotropy within the upper Precambrian lithosphere. Anisotropy with horizontally polarised shear waves propagating faster than vertically polarised ones (Vsh > Vsv) is observed in the lower crust and mantle lithosphere and indicates horizontally oriented fabric. Anisotropy with Vsh < Vsv is observed in the upper crust beneath a number of locations and suggests the occurrence of vertically oriented fabric.

References

Lebedev, S., J. Boonen, J. Trampert, Seismic structure of Precambrian lithosphere: New constraints from broadband surface-wave dispersion, *Lithos*, Special Issue "Continental Lithospheric Mantle: the Petro-Geophysical Approach", 109, 96-111, 2009.

Lebedev, S., R. D. van der Hilst, Global upper-mantle tomography with the automated multimode inversion of surface and S-wave forms, *Geophys. J. Int., 173*, 505-518, 2008.

First Multi-Scale, Finite-Frequency Tomography Illuminates 3-D Anatomy of the Tibetan Plateau

Shu-Huei Hung *(National Taiwan University, Taiwan, R.O.C.),* **Wang-Ping Chen** *(University of Illinois, Urbana-Champaign),* **Ling-Yun Chiao** *(National Taiwan University, Taiwan, R.O.C.)*

With a new multi-scale parameterization, 3-D images from finite-frequency seismic tomography, including the very first images beneath central Tibet from S-waves, reveal that regions of low electric resistivity in the crust, previously observed along active rifts in southern Tibet, correlate well with regions of low P- and S-wave speeds (V). However, such regions are not interconnected, indicating that a prevailing south-directed, channel-like crustal flow seems inactive or this popular geodynamic model needs modification. In the upper mantle, there is no clear indication of regional down-welling between depths of 100 to 400 km. Instead, a strong, lateral boundary between high and low V extends up to 33°N, marking the northern limit of sub-horizontally advancing Indian lithospheric mantle.

References

Hung, S.-H., W.-P. Chen, L.-Y. Chiao and T.-L. Tseng, First multi-scale, finite-frequency tomography illuminates 3-D anatomy of the Tibetan plateau, *Geophys. Res. Lett., 37*, doi:10.1029/2009GL041875 (with on-line supplements), 2010.

Acknowledgements: We thank S.-L. Chung for helpful discussions, L. Zhao, an anonymous referee, and the Editor for their comments that help improve the manuscript. This work was supported by National Science Council of Taiwan grants 96-2119-M-002-016 and 97-2745-M-002-011 (S.-H.H.) and U.S. National Science Foundation grants EAR99-09362 ("Hi-CLIMB"), EAR05-51995, and EAR06-35419 (W.-P.C.)

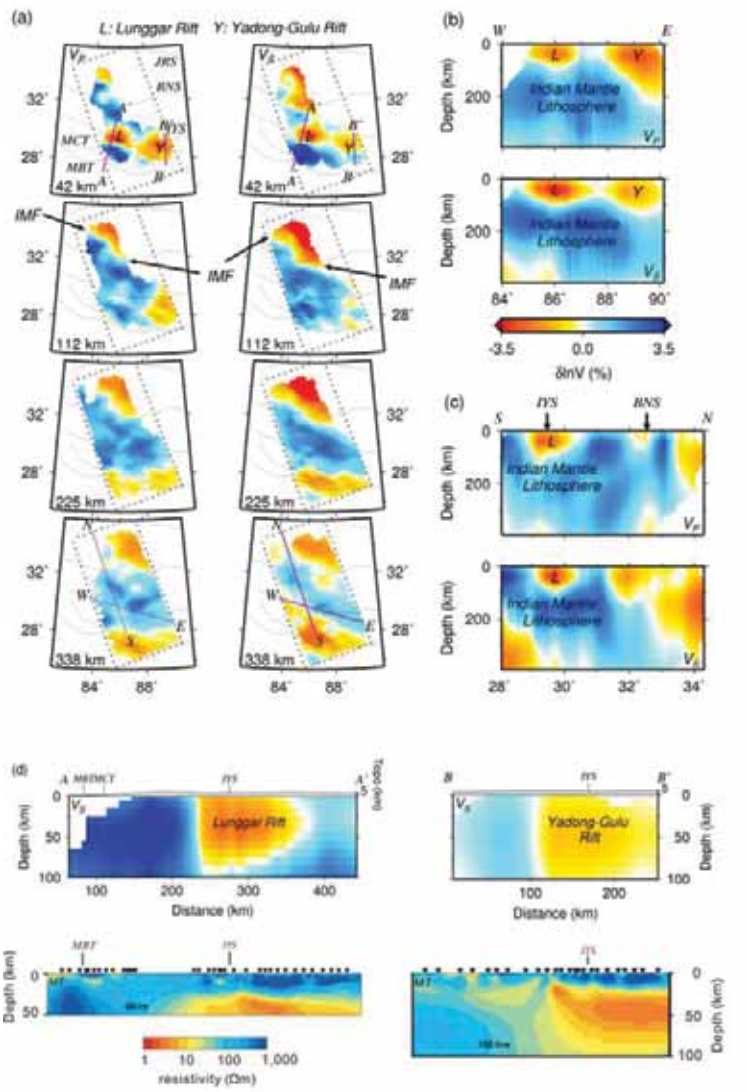

A map showing color-coded topography of the Himalayan-Tibetan collision zone. Finite-frequency travel-times recorded by 108 broadband stations (green triangles) are used to obtain multi-scaled, tomographic images for a large volume beneath western Tibet (box outlined by dashed lines). Blue solid lines indicate locations of profiles along which cross-sections of $\delta \ln V_P$ and $\delta \ln V_S$ are shown in Figure 3b and 3c. Blue dashed lines mark profiles across the Lunggar and the Yadong-Gulu rifts where profiles of electric resistivity are inferred from magnetotelluric (MT) measurements (at locations shown as purple open circles) and being directly compared with our results of $\delta \ln V_S$ in Figure 3d. For reference, positions of other temporary seismic stations, located to the east of our region of study and whose data were used to construct the tomographic profile of Tilmann et al. [2003], are also plotted (brown dashed line and orange inverted triangles). Other features not explained in the legend are: Young or active normal faults (red curves, Taylor and Yin [2009]); major geologic boundaries (solid curves), including (from north to south) JRS, the Jinsha River Suture; BNS, the Bangong-Nujiang Suture; IYS, the Indus-Yarlung Suture; STD, the South Tibet Detachment System; MCT, the Main Central Thrust; and MBT, the Main Boundary Thrust.

Seismic Structure of the Crust and the Upper Mantle beneath the Himalayas

Gaspar Monsalve (University of Colorado at Boulder), **Anne Sheehan** (University of Colorado at Boulder)

Seismic structure of the crust and the upper mantle beneath the Himalayas: Evidence for eclogitization of lower crustal rocks in the Indian Plate G. Monsalve, A. Sheehan, C. Rowe, and S. Rajaure Variations in the seismic velocity structure of the Himalayan collision zone include significant differences between its north and south portions, with transitions in physical properties across the Greater Himalaya. We combined P- and S-wave traveltimes from a temporary broadband seismic network in eastern Nepal and southern Tibet with arrival times at the permanent station network of the Department of Mines and Geology of Nepal to determine the seismic velocity structure across the Himalaya, using local earthquake tomography and traveltimes of regional earthquakes. The P-to-S velocity ratio (Vp/Vs) structure marks the difference between the Indian Plate and the overlying materials, with the Vp/Vs ratios being high for the former and low for the latter. We also found a significant increase in the uppermost mantle seismic velocities from south to north, reaching P-wave velocities (Vp) over 8.4 km/s north of the Greater Himalaya. These high Vp values do not seem to be the result of biases due to anisotropy in the upper mantle beneath the Greater and Tethyan Himalayas. Instead, we suggest that rocks in the lower crust of the underthrusting Indian Plate undergo metamorphism to eclogite as they plunge to greater depth beneath the mountain range, explaining the high seismic velocities.

References

Monsalve, G., A. Sheehan, C. Rowe, and S. Rajaure (2008), Seismic structure of the crust and the upper mantle beneath the Himalayas: Evidence for eclogitization of lower crustal rocks in the Indian Plate, *J. Geophys. Res., 113,* B08315, doi:10.1029/2007JB005424.

Acknowledgements: Broadband seismometers used in this experiment are from the IRIS PASSCAL program and data are archived at the IRIS DMC. We thank the staff of the Department of Mines and Geology of Nepal for their assistance with the experiment and for sharing their network seismic data with us. This work was supported by grants from the National Science Foundation and the Department of Energy.

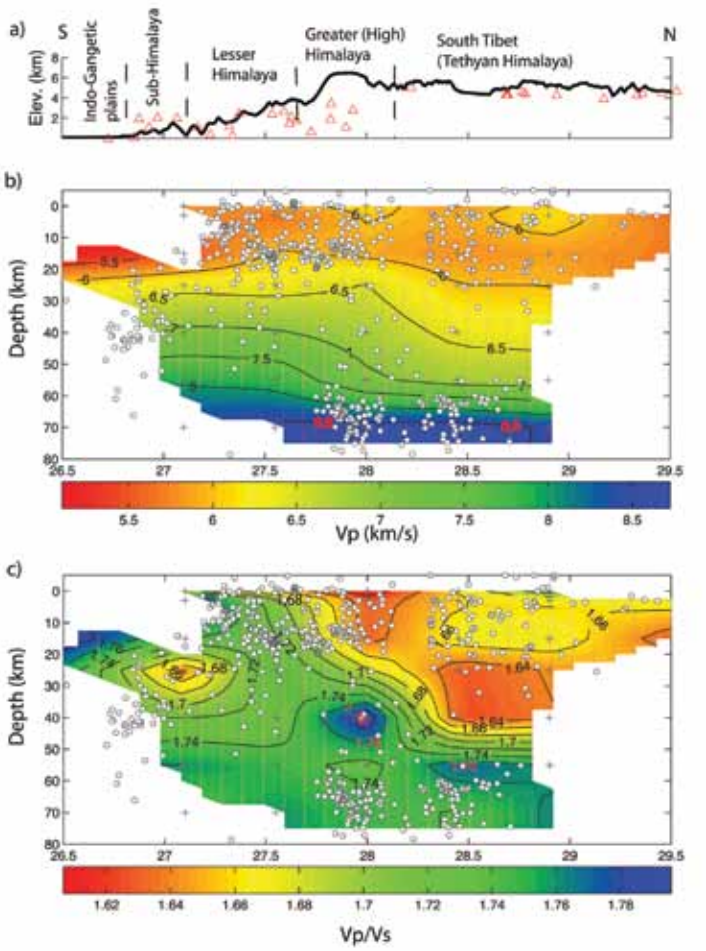

Two-dimensional north-south structure of Vp and Vp/Vs beneath eastern Nepal and the southern Tibetan Plateau. Earthquakes are projected onto an N-S cross-section. (a) North-south topographic cross-section at 86.5°E, red triangles denote projected station locations. (b) North-south Vp structure. Horizontal axis is latitude in degrees North. (c) North-south Vp/Vs structure.

Evolution of Caribbean – South American Plate Boundary from Surface Wave Tomography

Meghan S. Miller *(University of Southern California),* **Alan Levander** *(Rice University),* **Fenglin Niu** *(Rice University)*

We have measured shear wave velocity structure of the crust and upper mantle of the Caribbean – South American boundary region by analysis of fundamental mode Rayleigh waves in the 20-100s period band recorded at the BOLIVAR/GEODINOS stations from 2003 to 2005. The model shows lateral variations that primarily correspond to tectonic provinces and boundaries. A clear linear velocity change parallels the plate bounding dextral strike-slip fault system along the northern coast of Venezuela, illustrating the differences between the South American continental lithosphere, the Venezuelan archipelago, and the Caribbean oceanic lithosphere. At depths up to 120 kilometers beneath the Venezuelan Andes and the Maracaibo block there is evidence of underthrusting of the Caribbean plate, but there is no other evidence of subduction of the Caribbean plate beneath the South American plate. In eastern Venezuela linear crustal low velocities are associated with the fold and thrust belts whereas as higher crustal velocities are imaged in the Guayana shield lithosphere. The subducting oceanic part of the South American plate is imaged beneath the Antilles Arc. The surface wave images combined with seismicity data suggest shear tearing of the oceanic lithosphere away from the buoyant continental South American plate offshore of northeastern Venezuela. The continental lithosphere south of the slab tear is bent down towards the plate boundary in response to the propagating tear in the lithosphere. We interpret a nearly vertical low velocity "column" west of the tear centered beneath the Cariaco Basin, with three dimensional asthenospheric flow around the southern edge of the subducting oceanic lithosphere, with the asthenosphere escaping from beneath continental South America, and rising into the plate boundary zone. The complex plate boundary structure is best examined in three-dimensions. We discuss the new surface wave tomographic inversion in the context of results from other researchers including local seismicity, teleseismic shear wave splits, and interpretations from active source profiling.

Acknowledgements: BOLIVAR was funded by grants EAR0003572 and EAR0607801 from the NSF Continental Dynamics Program, and funding to our Venezuelan colleagues from CONICIT, the Venezuela Science Foundation, and PDVSA.

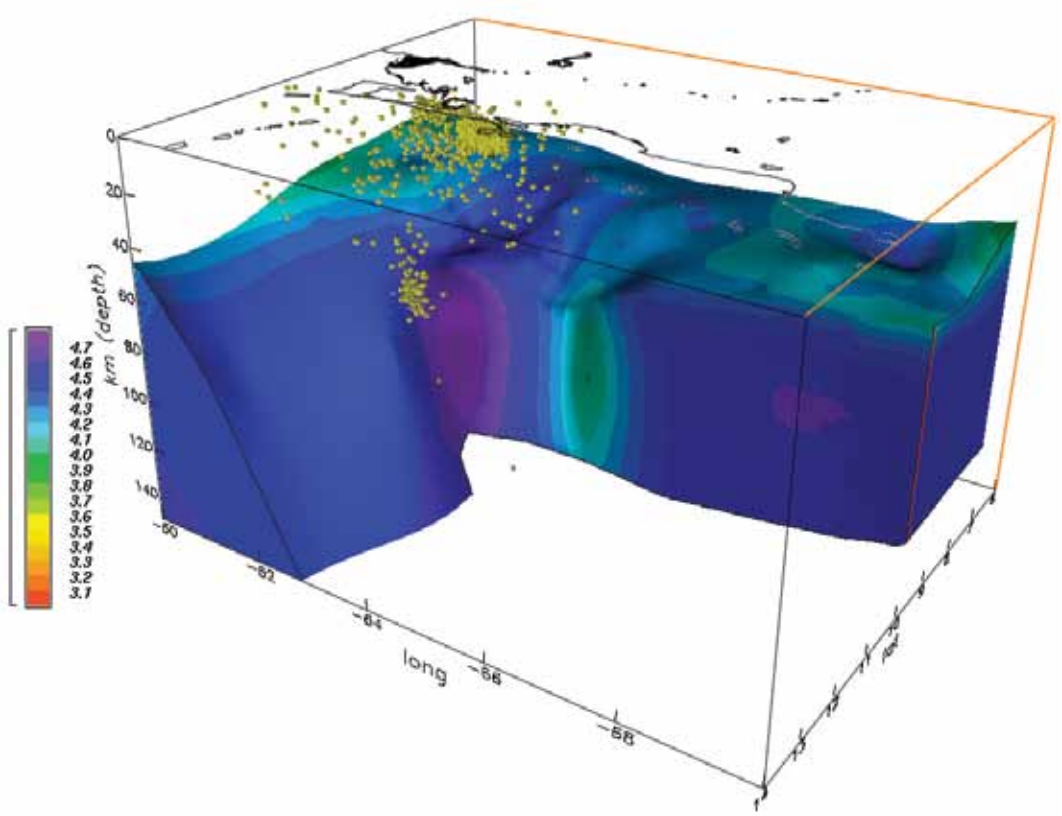

Surface wave tomography model illustrating the structure of the South American mantle lithosphere as viewed from the northwest. The yellow dots are relocated seismicity, which define the Paria cluster and the location of the subducted oceanic lithosphere beneath the Antilles arc tearing away from the continental lithosphere along the Caribbean-South American plate boundary.

Subducted Oceanic Asthenosphere and Upper Mantle Flow beneath the Juan de Fuca Slab

R. M. Russo *(University of Florida)*

Many studies have shown that typical oceanic lithosphere is underlain by a well developed asthenosphere characterized by slow seismic velocities from ~100-250 km depth. However, the fate of the oceanic asthenosphere at subduction zones is poorly understood. I show here using shear wave splitting of S waves emanating from earthquakes in the Juan de Fuca slab that upper mantle asthenospheric anisotropy beneath the slab is consistent with the presence of two distinct subducted asthenospheric layers, one with fast shear trends parallel to the subduction trench, and a second, deeper layer with fast upper mantle fabrics parallel to the motion of the Juan de Fuca plate with respect to the deeper mantle. The consistent orientation of unsubducted Pacific asthenospheric anisotropy in the direction of current plate motion implies that the trench-parallel sub-slab anisotropy develops when the lithosphere subducts.

References

Russo, R. M., Subducted oceanic asthenosphere and upper mantle flow beneath the Juan de Fuca slab, *Lithosphere, 1,* 195-205, 2009.

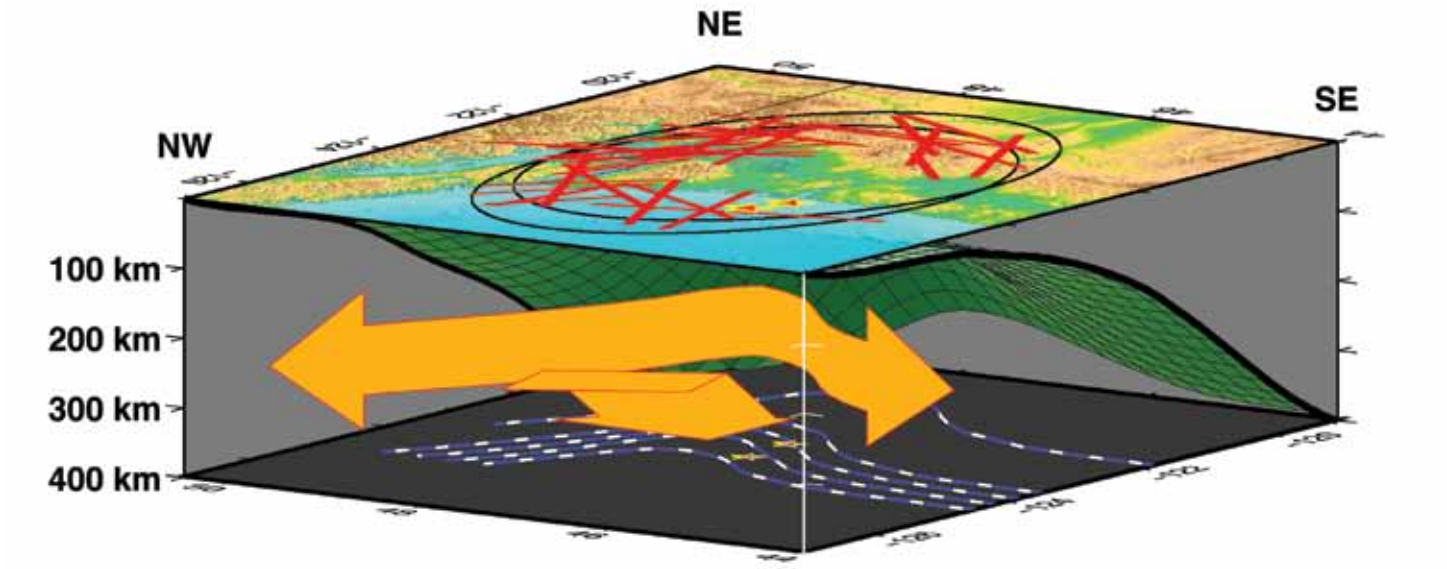

Block diagram showing Juan de Fuca slab geometry (green meshed surface), and top-of-slab depth contours (heavy blue dashed lines, bottom). Source side S splitting measurements are compatible with presence of two anisotropic layers beneath the Juan de Fuca slab: a layer immediately beneath the slab which is characterized by trench-parallel fast shear azimuths, and a deeper layer with fast shear trends parallel to the motion of the Juan de Fuca plate with respect to assumed fixed hotspots (Gripp and Gordon, 2003). Orange arrows schematically show the anisotropy and possibly upper mantle flow directions in these two layers.

Subduction of the Chile Ridge: Upper Mantle Structure and Flow

R. M. Russo *(University of Florida),* **J. C. VanDecar** *(DTM - Carnegie Inst. Washington),* **D. Comte** *(Universidad de Chile),* **V. I. Mocanu** *(University of Bucharest),* **A. Gallego** *(University of Florida),* **R. E. Murdie** *(Goldfields Australia)*

We deployed 39 broadband seismometers in southern Chile from Dec. 2004 to Feb. 2007 to determine lithosphere and upper mantle structure, including possible slab windows, in the vicinity of the subducting Chile Ridge. Body-wave travel-time tomography clearly shows the existence of a long-hypothesized slab window, a gap between the subducted Nazca and Antarctic lithospheres. P-wave velocities in the slab window are distinctly slow relative to surrounding asthenospheric mantle. Thus, the gap between slabs visible in the imaging appears to be filled by unusually warm asthenosphere, consistent with subduction of the Chile Ridge. Shear-wave splitting in the Chile Ridge subduction region is very strong (mean delay time nearly ~3 s) and highly variable. North of the slab window, splitting fast directions are mostly trench parallel, but, in the region of the slab gap, splitting fast trends appear to fan from NW-SE trends to the north, through ENE-WSW trends toward the middle of the slab window, to NE-SW trends south of the slab window. We interpret these results as

indicating flow of asthenospheric upper mantle into the slab window.

References

Russo, R. M., J.C. VanDecar, D. Comte, V.I. Mocanu, A. Gallego, and R.E. Murdie, Subduction of the Chile Ridge: Upper Mantle Structure and Flow, *GSA Today, 20* (9), 4-10, doi: 10.1130/GSATG61A.1, 2010.

Acknowledgements: Supported by U.S. National Science Foundation grant EAR-0126244 and CONICYT grant no. 1050367 from the government of Chile.

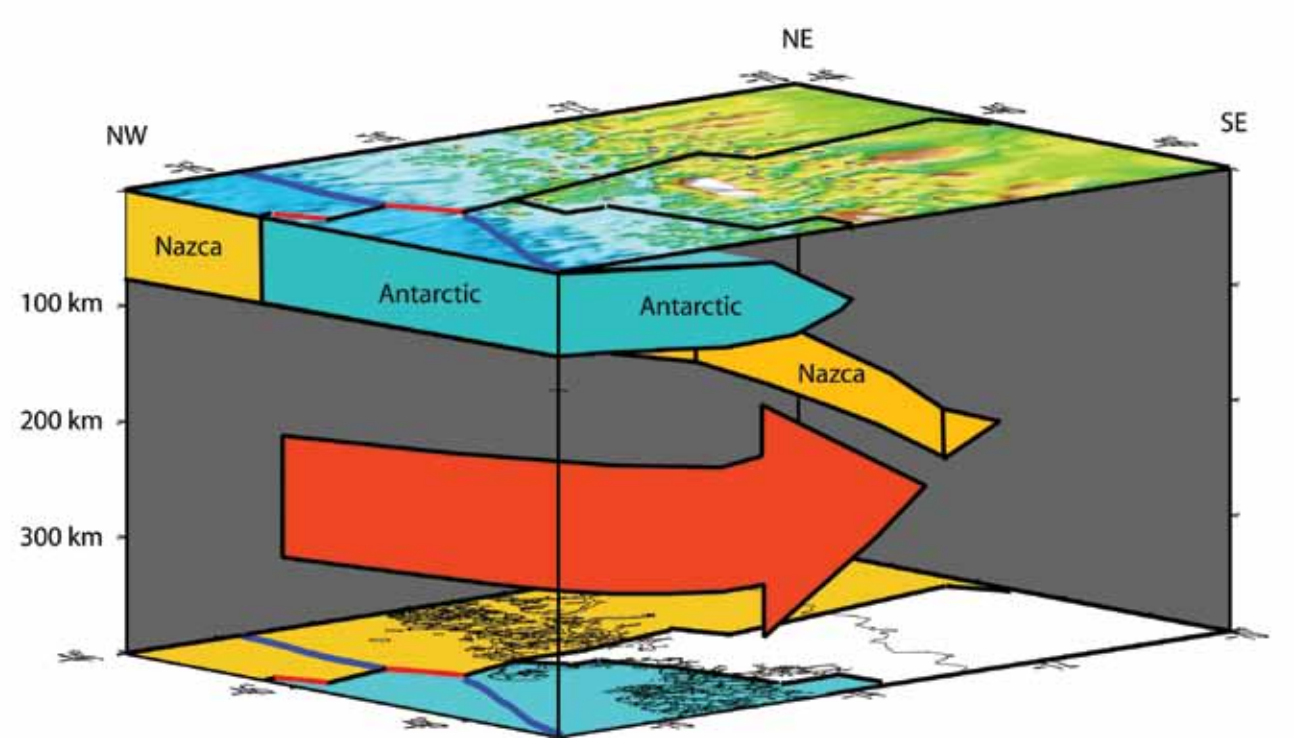

Schematic 3-d block diagram of upper mantle flow in the vicinity of the slab window delineated by the travel time inversions. Map on top of block shows relief and locations of Chile Ridge structures before subduction and after. Bottom of block shows coastline and Chile Ridge structures over color-coded slab plates: Nazca plate in dark yellow, Antarctic plate in blue-green. Same colors for portions of slab visible in the block diagram itself. Red arrow parallels shear wave splitting fast trends and upper mantle flow in the vicinity of the slab window opening. View from the SW, looking NE. Note the northern, shallower portion of the slab window is not visible from this viewpoint.

Detecting the Limit of Slab Break-off in Central Turkey: New High-resolution Pn Tomography Results

C.R. Gans *(University of Arizona),* **S.L. Beck** *(University of Arizona),* **G. Zandt** *(University of Arizona),* **C.B. Biryol** *(University of Arizona),* **A.A. Ozacar** *(Middle East Technical University)*

Inversion of Pn travel time residuals from a 39-station portable broadband array (instruments provided by IRIS PASSCAL) provides a high-resolution image of the velocity structure in the uppermost mantle beneath central Turkey. Individually picked Pn phase arrivals from events recorded by the North Anatolian Fault Passive Seismic Experiment and the Kandilli Observatory were combined with additional events associated with the Eastern Turkey Seismic Experiment. Tomography results show no change in Pn velocity across the North Anatolian Fault, although longitudinal variations are evident. A region of very low Pn velocities (< 7.8 km/s) is imaged east of the Central Anatolian Fault Zone (CAFZ), with a transition to faster velocities (> 8.1 km/s) west of the fault. The sharp transition along the CAFZ, which follows the paleotectonic Inner Tauride Suture, may represent the location of the edge of the slab window, created when the oceanic slab broke off along the Bitlis-Zagros Suture around 11 Ma, as the Arabian plate collided with the Eurasian plate.

References

Faccenna, C., Bellier, O., Martinod, J., Piromallo, C. and V. Regard (2006), Slab detachment beneath eastern Anatolia: A possible cause for the formation of the North Anatolian fault, *Earth Planet. Sci. Lett., 242*, 85-97.

Acknowledgements: National Science Foundation Grant EAR0309838

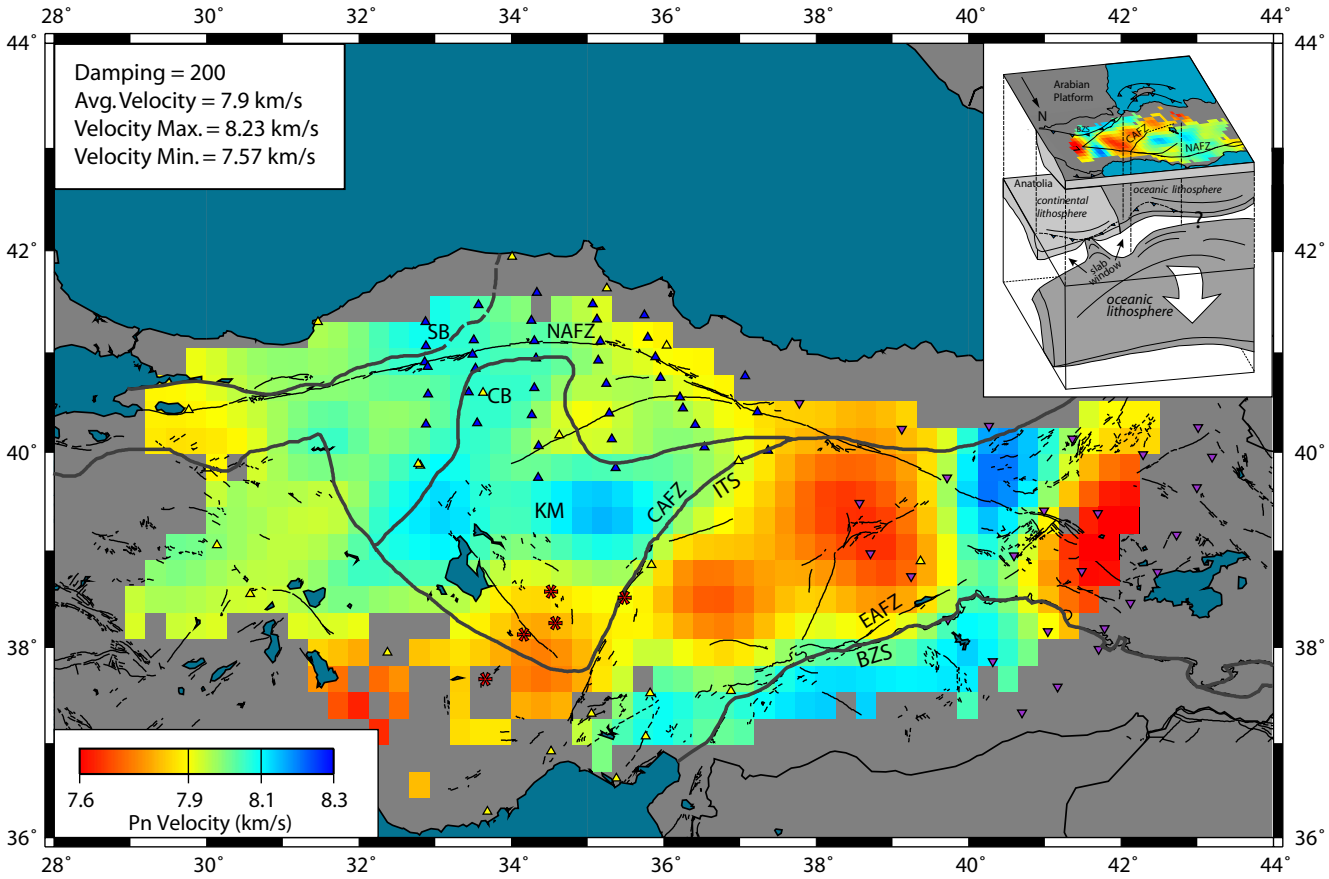

Figure 1. Pn tomography results for north-central Turkey. Stations shown by triangles, Holocene volcanoes by red asterisks. NAFZ - North Anatolian Fault Zone, CAFZ - Central Anatolian Fault Zone, EAFZ - East Anatolian Fault Zone, ITS - Inner Tauride Suture, KM - Kirsehir massif, SB - Safranbolu Basin, CB - Cankiri Basin, BZS - Bitlis Zagros Suture. Red asterisks are Holocene volcanoes. Inset: Cartoon showing hypothesized upper mantle slab detachment and resulting slab window consistent with Pn tomography results. The downdip edge of the slab window corresponds to the northern edge of the low Pn region that partially follows the CAFZ. The western extent of the tear is uncertain. Modified after Faccenna et al. [2006].

Imaging the Flat Slab Beneath the Sierras Pampeanas, Argentina, Using Receiver Functions: Evidence for Overthickened and Broken Subducted Oceanic Crust

C.R. Gans *(University of Arizona),* **S.L. Beck** *(University of Arizona),* **G. Zandt** *(University of Arizona),* **H. Gilbert** *(Purdue University),* **P. Alvarado** *(Universidad Nacional de San Juan, Argentina)*

The western margin of South America between 30° and 32° S is characterized by the flat slab subduction of the ~43 Ma oceanic Nazca plate beneath the continental South American plate. Several arrays of PASSCAL broadband seismic instruments have been deployed in Chile and western Argentina to study this phenomenon (e.g., CHARGE, 2000-2002; SIEMBRA, 2007-2009; ESP, 2008-2010). The low angle subduction has prevented magmatism in the area since the late Miocene, and spatially correlates with the formation of both thick-skinned (Sierras Pampeanas) basement cored uplifts and the thin-skinned (Andean Precordillera) fold and thrust belt within the region. In order to better constrain the crust and upper mantle structure in the transition region between flat slab and normal subduction to the south, we have calculated receiver functions (RFs) from teleseismic earthquakes. Using our dense SIEMBRA array, combined with the broader CHARGE and ESP arrays, we are able to image in detail the flat slab, which contains a distinct negative arrival (indicative of a low velocity zone) at the top of the flat slab, followed by a strong positive P-to-S conversion. While the exact causes of flat slab subduction continue to be debated, one overriding theme is the necessity of having an overthickened crust in order to increase the buoyancy of the subducting slab. In this region, the hotspot seamount chain of the Juan Fernandez Ridge (JFR) is thought to provide such a mechanism. Kopp et al. [2004], however, did not find overthickened crust in the offshore portion of the JFR, but rather only moderately thick oceanic crust. Preliminary results from our RFs, compared with synthetic RFs, indicate that the oceanic crust at the top of the slab (the low velocity zone) must be at least ~12-14 km thick. Our results support the idea of an overthickened crust in the subducted flat slab beneath western Argentina. Further, there are indications in the receiver functions that the subducted oceanic crust in the region directly along the path of the subducted ridge is broken by trench parallel faults. One explanation for this could be that these are older faults in the oceanic crust, created when the crust was first subducted. Alternatively, it is possible that new faults are forming due to stresses induced by increased coupling in the flat slab region.

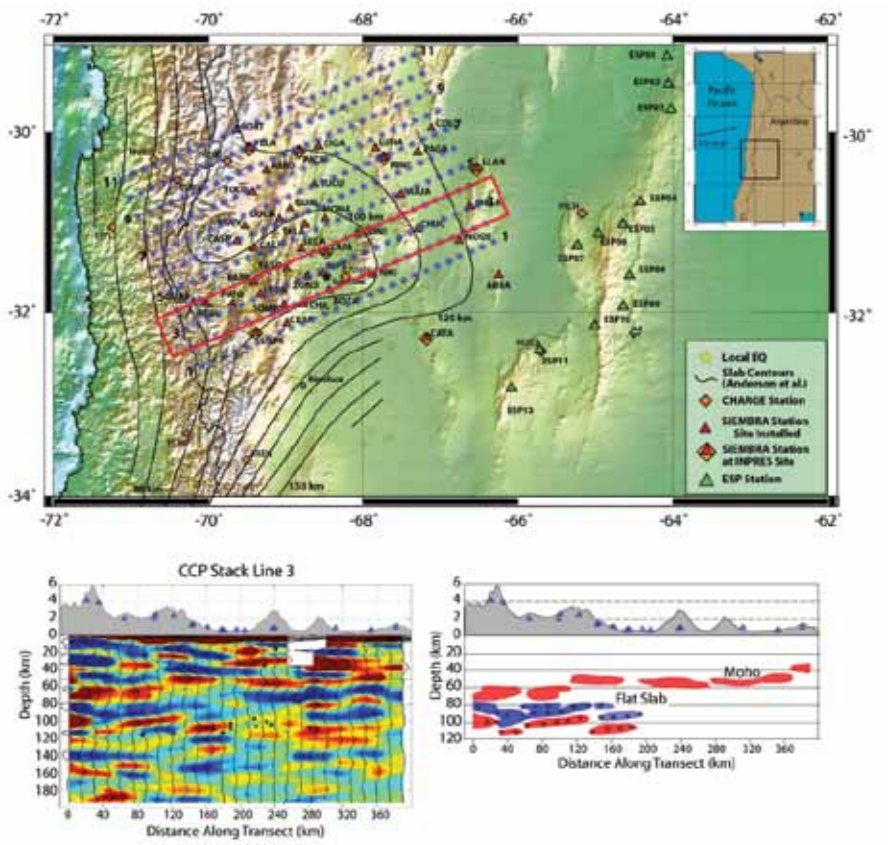

Top: Location map with PASSCAL stations and nodes for Common Conversion Point (CCP) mesh. Bottom: Line 3, along the direct line of the JFR. Note the complex and broken character of the oceanic crust. Blue triangles are seismic stations, black circles are slab earthquakes recorded during SIEMBRA.

References

Kopp, H., Flueh, E.R., Papenberg, C. and D. Klaeschen (2004), Seismic investigations of the O'Higgens Seamount Group and Juan Fernandez Ridge: Aseismic ridge emplacement and lithosphere hydration, *Tectonics, 23*

Acknowledgements: National Science Foundation Grant # EAR-0510966.

Pn Tomography of the Western United States using USArray

Janine Buehler *(SIO, University of California, San Diego),* **Peter Shearer** *(SIO, University of California, San Diego)*

In this study, we analyze Pn arrival times from the transportable stations of USArray to resolve crust and uppermost-mantle structure. Seismic tomography has the potential to provide detailed images of Earth structure, but is often limited by the coverage of the available seismic data. The USArray with its very dense and almost uniformly spaced stations has greatly improved tomographic resolution for much of the western United States. Because of the large contrast in seismic velocities between the lower crust and the upper mantle and the shallow velocity gradient in the upper mantle, Pn tomographic velocity perturbation images show results for a very confined depth in the uppermost mantle, complementing surface-wave or other body-wave tomographies that average anomalies over larger depth intervals.

Acknowledgements: We thank Luciana Astiz and the operators of the Array Network Facility for making their phase picks available. This research was funded by grant EAR-0710881 from the National Science Foundation.

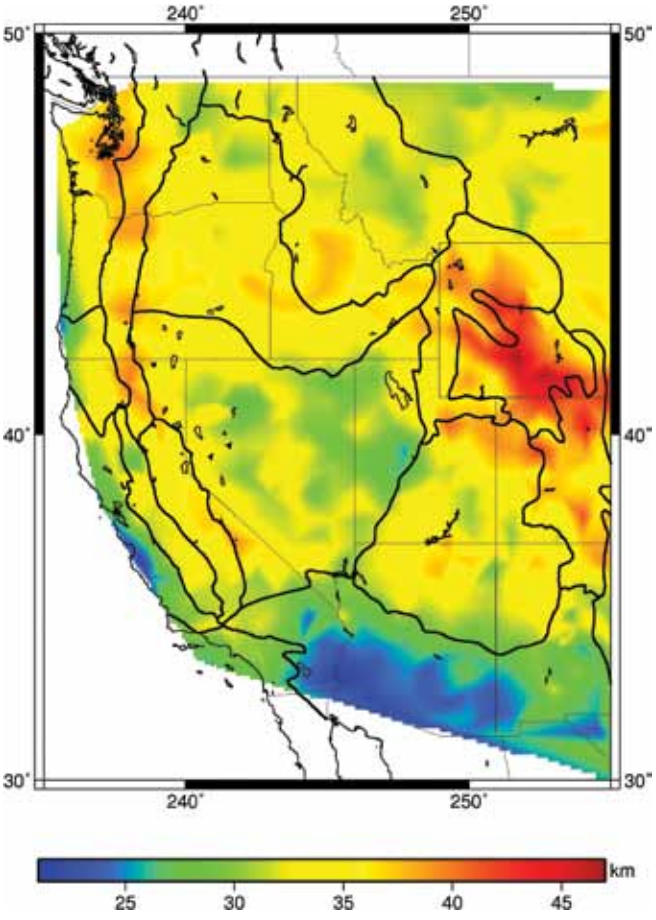

Crustal thickness estimates. Thicker crust is observed in the Sierra Nevada, the Cascade Range, and southern Wyoming. In the northern Basin and Range province crustal thickness is reduced as expected in an extensional tectonic regime. The thinner crust in the southern Basin and Range is very distinct, with thicker crust indicated to the north below the Colorado Plateau.

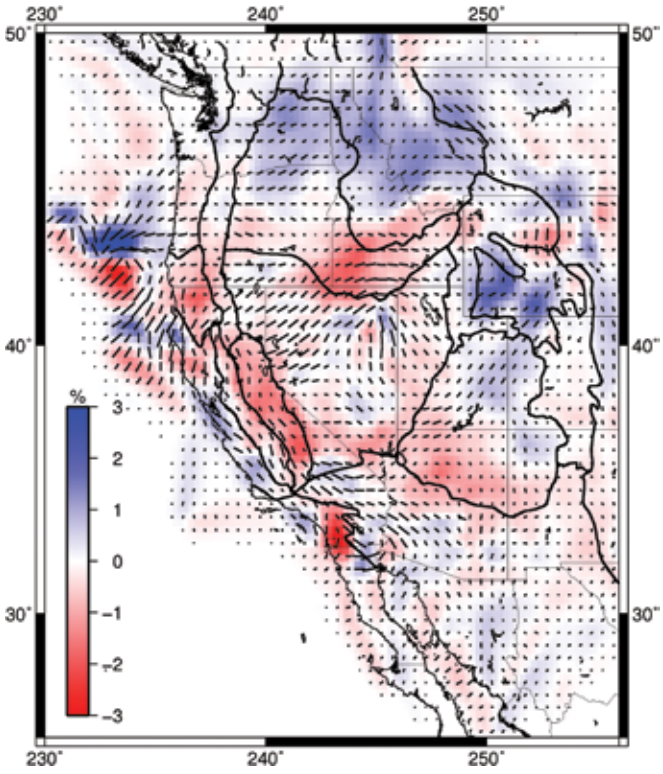

Isotropic velocity perturbations resulting from a combined iso-anisotropic inversion. Red colors indicate areas of lower velocities and blue colors regions with higher velocities. The locations of the major anomalies correlate well with known active processes, as for example the large low velocity anomalies in the Snake River Plain leading to the Yellowstone hotspot. The black lines indicate the Pn fast axis with the length of the line proportional to the strength of the anisotropy. We obtain large anisotropic anomalies in the Great Basin desert, off the coast of northern California, and in southern California/northern Mexico.

Geophysical Detection of Relict Metasomatism from an Archean (~3.5 Ga) Subduction Zone

Chin-Wu Chen (Carnegie Institution of Washington), **Stephane Rondenay** *(Massachusetts Institute of Technology),* **Rob. Evans** *(Woods Hole Oceanographic Institution),* **David Snyder** *(Geological Survey of Canada)*

The origin of Archean cratonic lithosphere is the subject of much debate. Geological and geochemical data are consistent with a plate tectonic origin involving assembly of predominantly oceanic terranes and micro continents into large stable cratons. Deep probing geophysical surveys of Archean cratons provide a means of understanding the processes responsible for the formation of these earliest continents, although the signals are complex and present-day cratons are only the surviving remnants of once larger entities. Here we present a unique geophysical view of structure within the Archean Slave craton, in northwestern Canada, that shows clear evidence for subduction processes frozen into Archean lithosphere. New seismic imaging results from the central Slave are synthesized with a coincident magnetotelluric model, and interpreted using petrological and geochemical constraints from mantle xenoliths. We find the most striking correlation between seismic and electrical structures ever observed in a continental setting in the form of a coincident seismic discontinuity and electrical conductor at ~100 km depth. The magnitude of both anomalies, in conjunction with the occurrence of phlogopite rich xenoliths originating at the same depth, point to a metasomatic origin. We believe that fluids were released from a subducting slab and altered the mantle directly below the base of a pre-cratonic lithosphere. Our model suggests that cratons are formed by subduction underplating and accretion of pre-existing fragments, and that these processes were active as early as 3.5 billion years ago.

References

Chen, C.-W., S. Rondenay, R. L. Evans, and D. B. Snyder, Geophysical detection of relict metasomatism from an Archean (~3.5 Ga) subduction zone, *Science, 326*, 1089-1091, 2009.

Jones, A.G., P. Lezaeta, I.J. Ferguson, A.D. Chave, R. L. Evans, X. Garcia and J. Spratt, The electrical structure of the Slave craton. *Lithos, 71*, 505-527, 2003.

Acknowledgements: This work is funded by the POLARIS consortium and NSF grant EAR-0409509 (S. R.).

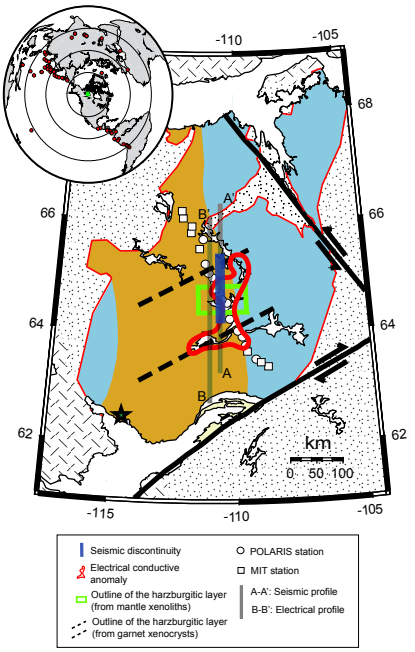

Map of the Slave craton (exposed craton outlined in red). Inset shows the craton in center (green square), with the 62 earthquakes (red circles) used for the analysis. Crustal topology and geochemical signatures broadly subdivide the Slave craton into two distinct regions: The older (4.03-2.83 Ga) Central Slave Basement Complex to the west (brown), and isotopically juvenile rocks (2.67-2.6 Ga) to the east (blue). The lateral extent of an ultra-depleted harzburgitic layer of the mantle lithosphere has been inferred from petrological analysis of mantle xenoliths (green outline) and geochemical analyses of garnet xenocrysts (between black dashed lines). The seismic stations are from POLARIS (circles) and MIT (squares). A-A' marks the location of the seismic profile shown in Fig. 2. The lateral extent of the seismic discontinuity is indicated by blue shading, and that of the conductive anomaly is outlined in red. B-B' is the nominal projected location of the MT array.

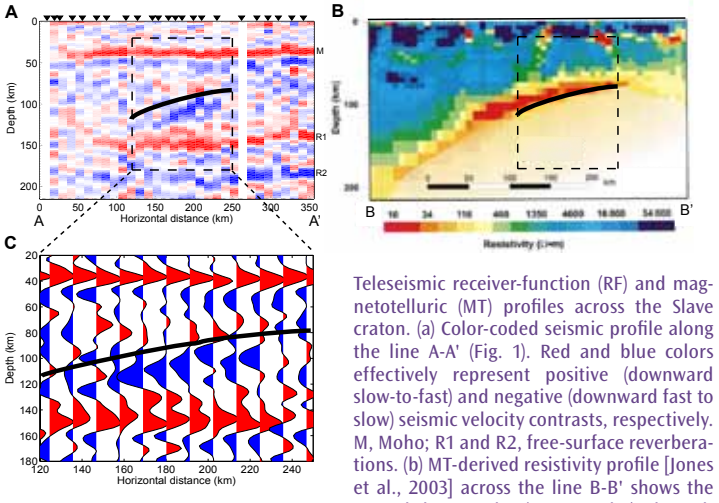

Teleseismic receiver-function (RF) and magnetotelluric (MT) profiles across the Slave craton. (a) Color-coded seismic profile along the line A-A' (Fig. 1). Red and blue colors effectively represent positive (downward slow-to-fast) and negative (downward fast to slow) seismic velocity contrasts, respectively. M, Moho; R1 and R2, free-surface reverberations. (b) MT-derived resistivity profile [Jones et al., 2003] across the line B-B' shows the central Slave conductive anomaly (red to yellow) at 80-120 depth. The solid black line highlights the base of the conductive anomaly within the region of interest (dashed black box), repeated to scale in RF profiles for comparison. (c) Close-up RF traces for bins in the region of interest.

3-D Isotropic Shear Velocity Model from Ambient Noise and Earthquake Tomography

Weisen Shen *(University of Colorado at Boulder),* **Yingjie Yang** *(University of Colorado at Boulder),* **Fan-Chi Lin** *(University of Colorado at Boulder),* **Michael H. Ritzwoller** *(University of Colorado at Boulder)*

Ambient Noise Tomography (ANT) is an efficient way to image the earth's crust since its inception in 2005. We use over 300,000 cross-correlations from ambient noise based on the past three years of EarthScope/USArray Transportable Array (TA) data. This data set provides empirical green's functions between each pair of stations and finally results in over 100,000 high SNR Rayleigh wave dispersion measurements from 8 and 40 sec period. Figure 1 shows the 12s Rayleigh wave velocity map with the Yellowstone hotspot and the principal sedimentary basins identified: CV (Central Valley), UB (Uinta Basin), GRB (Green River Basin), YS (Yellowstone), WB (Washakie Basin), PRB (Powder River Basin), DB (Denver Basin), AB (Albuquerque Basin), PB (Permian Basin), AB (Anadarko Basin). In addition, we perform surface wave tomography based on teleseismic earthquakes with the same station set using more than 200 earthquakes in two-plane-wave tomography (TPWT) to produce Rayleigh wave dispersion maps at from 25 to 144 sec. At In overlapping period band (25-40s) the two methods produce similar dispersion maps.

With these dispersion maps from 8 to 144 sec period, we apply Monte-Carlo inversion to construct a 3-D shear velocity model on the western US and the transition region to cratonic North America. Figure 2 shows a cross section of the 3model along 40oN in which geological provinces are shown: BR (Basin and Range), CP (Colorado Plateau), RM (Rocky Mountains), and GP (Great Plains). Low velocities are observed in the Great Plains and the northern Colorado plateau in the shallow crust, which coincides with sedimentary basins. In the mantle, low velocity anomalies are observed beneath the entire Basin and Range province extending from 113oW to 120oW. High velocity anomalies beneath the Colorado Plateau and the Great Basin extend to the depth of ~150km, indicating thickened lithosphere. The high horizontal velocity gradient along the Rocky Mountain front reveals the boundary between the tectonic western US and the cratonic eastern US. Future work will assimilate body wave information (receiver functions) and geothermal information to reduce the crustal thickness-velocity trade-off.

References

Yang, Y., M. H. Ritzwoller, F.-C. Lin, M. P. Moschetti, and N. M. Shapiro (2008), Structure of the crust and uppermost mantle beneath the western United States revealed by ambient noise and earthquake tomography, *J. Geophys. Res., 113*, B12310

Acknowledgements: All data used were obtained from the IRIS Data Management Center. The authors are grateful to Hersh Gilbert for providing the crustal thickness map.

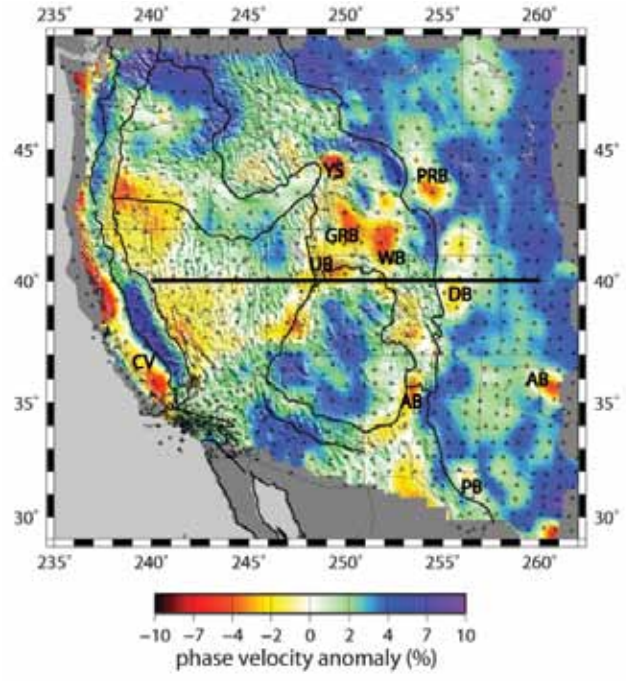

Figure1. Rayleigh wave phase velocity map derived from ANT at 12 s period where the main geological units are outlined with black contours and the principal sedimentary basins and hotspot are identified with abbreviations.

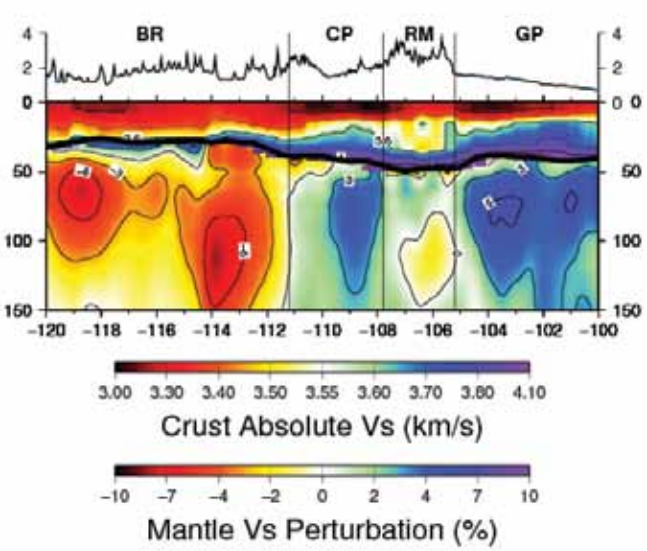

Figure2. Vertical cross section of shear wave velocity along 40°N delineated by the black line in Figure 1, where the crustal part is plotted as absolute shear velocity and the mantle is plotted as the shear velocity perturbation relative to the average velocity profile.

Shear-Wave Birefringence and Current Configuration of Converging Lithosphere under Tibet

Wang-Ping Chen *(University of Illinois, Urbana-Champaign),* **Michael Martin** *(University of Illinois, Urbana-Champaign)*

New data from west-central Tibet show that birefringence of S-waves has two pronounced increases in magnitude toward the hinterland. Null birefringence persists to about 75 km north of the Indus-Yarlung suture (IYS) between the Indian shield and the Lhasa terrane of southern Tibet. A second, rapid increase occurs about 100 km farther north of the Bangong-Nujiang sutures between the Lhasa terrane and the Qiangtang terrane in central Tibet. The latter feature is consistently observed along three long transects that collectively span a lateral (orogen-parallel) distance of about 600 km and is likely to mark the northern, leading edge of sub-horizontally advancing mantle lithosphere of the Indian shield (the "Greater India") – an interpretation consistent with the latest results of finite-frequency tomography using both P- and S-wave travel-times, previous results of modeling gravity anomalies, and a host of other seismic observations. Similarly, complementary constraints indicate that the sudden onset of significant birefringence north of the IYS is likely to be the southern termination of Eurasian mantle lithosphere. Curiously, the shortest of three transects showed null birefringence through much of the Lhasa terrane, a pattern inconsistent with those of He isotopes and gravity.

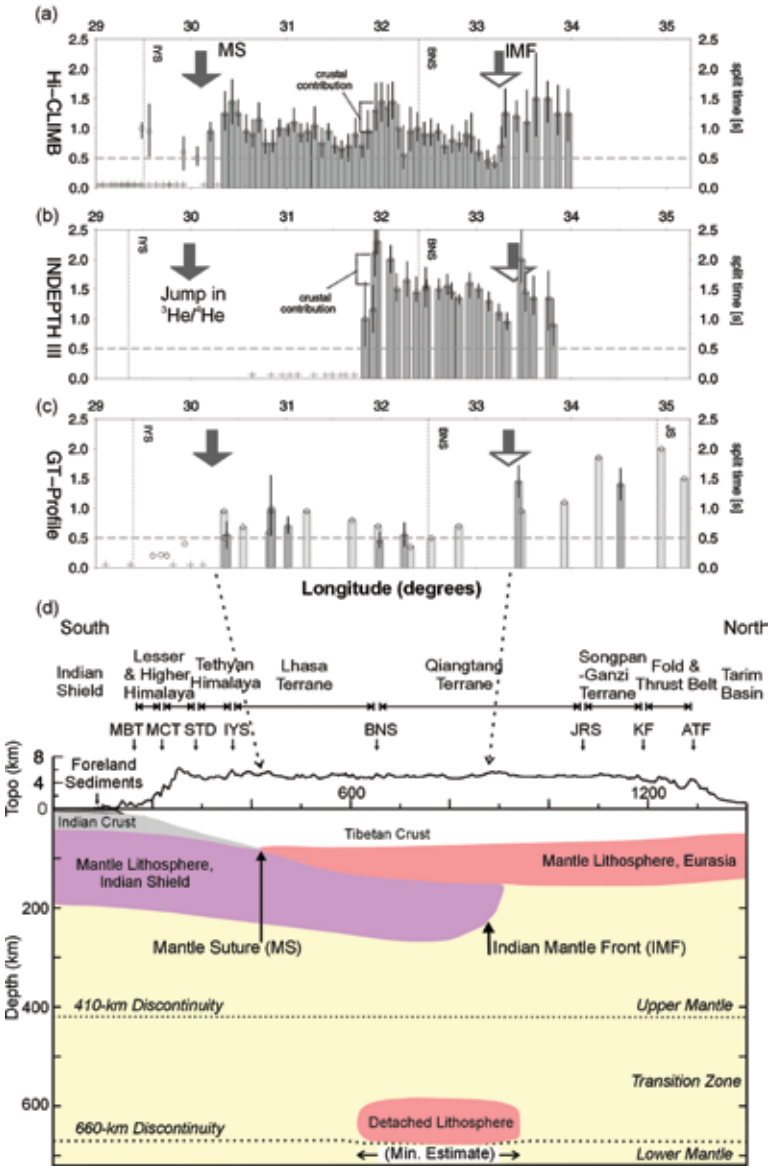

(a) to (c) Comparisons of three large-scale profiles of S-wave split time (*dt* in s) across Tibet. Open circles are isolated cases of birefringence south of the mantle suture. Measurements with error-bars (and shown in dark grey) are those analyzed by us; otherwise we plot values reported in the literature. The horizontal dotted-line represents the threshold for null birefringence. (d) A schematic cross-section showing the current configuration of the sub-continental lithospheric mantle, including a large-scale anomaly of high *P*-wave speed resting on top of the lower mantle and interpreted as the remnant of thickened (and subsequently detached due to Rayleigh-Taylor instability) lithospheric mantle (Chen and Tseng, 2007).

References

Chen, W.-P., M. Martin, T.-L. Tseng, R. L. Nowack, S.-H. Hung, and B.-S. Huang, Shear-wave birefringence and current configuration of converging lithosphere under Tibet, *Earth Planet. Sci. Lett., 295*(1-2), 297-304, doi:10.1016/j.epsl.2010.04.017, 2010

Chen, W.-P., and T.-L. Tseng, Small 660-km seismic discontinuity beneath Tibet implies resting ground for detached lithosphere, *J. Geophys. Res., 112*, B05309 (15 pp.), doi:10.1029/2006JB004607, 2007.

Acknowledgements: This work was supported by U.S. National Science Foundation grants EAR99-09362, EAR05-51995, EAR06-35419 (W.-P.C.), EAR EAR06-35611(R.L.N.), U.S. Air Force contract FA8718-08-C-002 (R.L.N. and W.-P.C.), National Science Council of Taiwan grants 96-2119-M-002-016 and 97-2745-M-002-011 (S.-H.H.), and Academia Sinica, Taiwan (B.-S.H.) which provided additional personnel (Wen-Tzong Liang, Chia-Lung Wu, John Lin, and Chun-Chi Liu). Seismic experiments were carried out jointly with Oregon State University (lead by John Nabelek), Chinese Academy of Geological Sciences (lead by Jiang Mei and Heping Su), Nepal Department of Mines and Geology (lead by Soma Sapkota and M. Pandey) and Peking University (lead by John Chen). We thank two anonymous reviewers for useful comments on the manuscript, F. Tilmann for discussions, and Zhaohui Yang (University of Illinois) for help with GIS databases.

Seismic Anisotropy Associated with Continental Lithosphere Accretion beneath the CANOE Array

Anna M. Courtier *(James Madison University),* **James B. Gaherty** *(Lamont-Doherty Earth Observatory),* **Justin Revenaugh** *(University of Minnesota),* **Michael G. Bostock** *(University of British Columbia),* **Edward J. Garnero** *(Arizona State University)*

The Canadian Northwest Experiment (CANOE) is an array of ~60 broadband seismometers located in northern Alberta and British Columbia and southern Yukon and Northwest Territories. The array spans nearly 4.0 Ga of geologic history, transitioning from the ancient craton in the east across the Canadian cordillera in the west. We examined anisotropy beneath the array using shear wave splitting of SKS, SKKS, and sSKS phases. Fast directions are roughly consistent with absolute plate motion across much of the array, suggesting that a coherent, asthenospheric fabric underlies the region. Variability in fast directions on smaller length scales (~50-200 km) generally correlates with surface structures and tectonic features, indicating a lithospheric contribution to the anisotropy. Within the craton, anomalous splitting is observed at an ancient suture zone and appears to stem from dipping fabric produced during continental assembly [*Mercier et al., 2008*]. The mantle signature of the craton-cordillera transition appears to coincide with the Rocky Mountain front, indicated by an abrupt change in fast directions. In the western cordillera, fast directions become parallel to the plate boundary, indicating that fabrics associated with the plate boundary deformation extend ~200 km into the continent. Splitting times average ~0.65 s across the array, though delay times are smaller across much of the cordillera. Smaller delay times indicate that anisotropy is weaker or less coherent across the cordillera relative to the craton.

References

Courtier, A.M., J.B. Gaherty, J. Revenaugh, M.G. Bostock, and E.J. Garnero (In Press). Seismic anisotropy associated with continental lithosphere accretion beneath the CANOE array, northwestern Canada, Geology.

Gripp, A.E., and R.G. Gordon (2002). Young tracks of hotspots and current plate velocities: *Geophys. J. Int., 150*, 321–361.

Mercier, J.-P., M.G. Bostock, P. Audet, J.B. Gaherty, E.J. Garnero, and J.S. Revenaugh (2008). The Teleseismic Signature of Fossil Subduction: Northwestern Canada, *J. Geophys. Res., 113*, B04308.

Acknowledgements: All data were obtained from the IRIS DMC; Data for CNSN stations were made available by the Geological Survey of Canada. Funding was provided by the National Science Foundation-Geophysics, the LITHOPROBE project, and a University of Minnesota Doctoral Dissertation Fellowship (AMC).

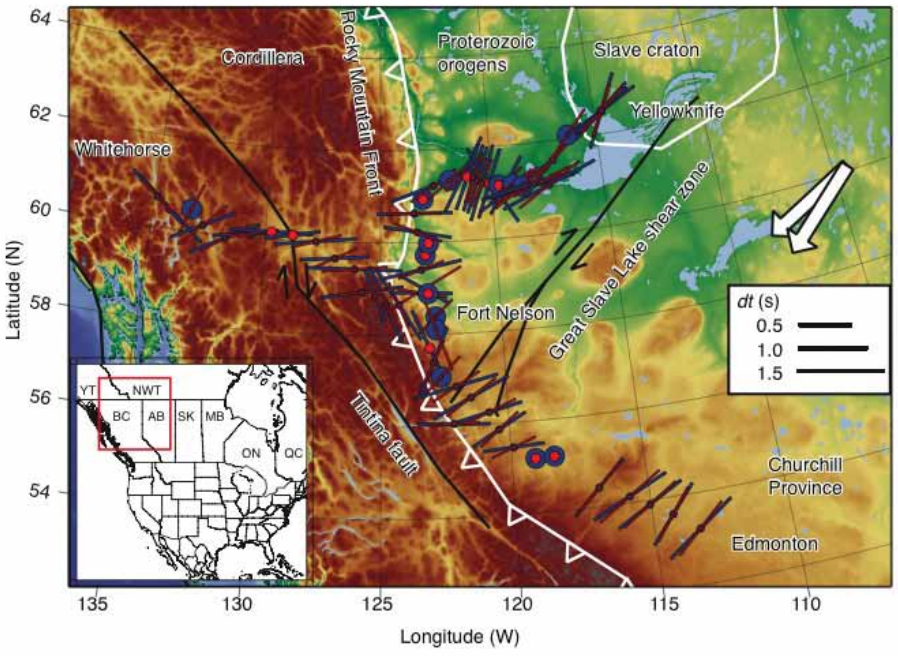

Regional geologic setting and multi-event station averages at CANOE and CNSN stations. Center of bar indicates station location; Length of bar indicates dt; Orientation of bars indicates fast direction (φ). Red = NE components, Blue = RT components. Uncertainty estimates are φ ±8° and dt ±0.2 s. Circles indicate null measurements; white arrows indicate plate motion from hot spot and no net rotation models (Gripp and Gordon, 2002).

Stratified Seismic Anisotropy beneath the East Central United States

Frédéric Deschamps (ETH Zurich), **Sergei Lebedev** *(DIAS Dublin),* **Thomas Meier** *(University Bochum),* **Jeannot Trampert** *(University Utrecht)*

A key problem in seismology is to resolve the radial distribution of azimuthal anisotropy beneath continents. Seismic anisotropy can be related to rock deformation that occurs during various geodynamical events, and can thus be used to better understand the deformation history of continental lithosphere. Array studies of azimuthal variations in surface-wave phase velocity are well suited to recover the radial distribution of anisotropy, provided that dispersion curves can be measured in a broad enough period range. Using about 20000 records from the IRIS database, we measured broadband inter-station dispersion curves of the Rayleigh-wave phase velocity and built an anisotropic Rayleigh-wave model that clearly resolves the radial distribution of azimuthal anisotropy beneath the East-central United States (31°-41° N and 82°-92° E) [Deschamps et al., 2008a]. We then estimated the amplitude of VS-anisotropy as a function of depth, from the lower crust to the upper asthenospheric mantle (≤400 km) [Deschamps et al., 2008b]. Beneath the orogenic terrains (south and east of the Grenville front), distinct patterns can be identified in three period ranges (Figure 1), suggesting that anisotropy is radially distributed within three distinct layers. At 20-35s (sampling the upper lithosphere), anisotropy is strong (~ 1% of the regional average isotropic velocity), with a direction of fast propagation sub-parallel to orogenic fronts. At 45-60s (sampling the lower lithosphere), anisotropy is moderate (~ 0.5%), and the direction of fast propagation is parallel to the reconstructed motion of the North-American plate 160-125 Ma ago. Finally, around 140s (sampling the upper asthenosphere), anisotropy is strong again (> 1%), and the direction of fast propagation is in good agreement with SKS splitting and with the absolute plate motion of North America. Beneath the cratonic terrains (north and west of the Grenville front), only the anisotropy at 140s, likely related to the current motion of the North American plate, is clearly visible. This distribution suggests the following scenario: ca 270 My ago, the upper lithosphere deformed during the final stages of the Appalachian orogeny (for instance, due to lateral extrusion), leading to fabrics that are now frozen and seen by Rayleigh wave azimuthal anisotropy at 20-35s. After the orogen, the hotter, softer, lower lithosphere recorded the motion of the North-America plate during a brief laps of time (160-125 Ma), resulting in fabrics that are now observed at 45-60s. Finally, at present time, the asthenospheric flow induces deformations at the top of the asthenosphere, which are mapped around140s.

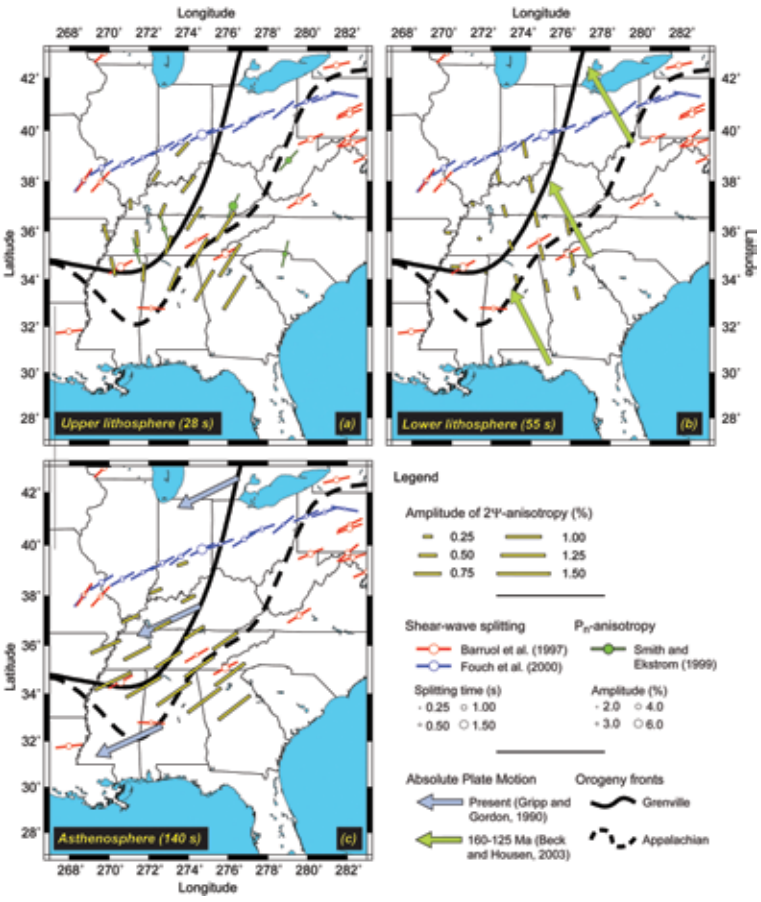

Rayleigh wave azimuthal anisotropy (yellow bars) at 28, 55, and 140 s. The orientation and size of the bar show the direction of fastest propagation of Rayleigh waves at the period and the amplitude of the anisotropy, respectively. Also plotted are main tectonic boundaries, past and present absolute plate motion, and previous anisotropy measurements. (a) At 28 s, the Rayleigh-wave fast-propagation direction beneath orogenic provinces is roughly parallel to the Grenville and Appalachian fronts, as well as to Pn fast-propagation direction. (b) At 55 s, the fast-propagation azimuth is close to the direction of the NNW drift of the North American plate during the Mesozoic. (c) At 140 s, the fast-propagation direction is parallel to the current absolute plate motion, as well as to most fast-propagation directions inferred from shear-wave splitting observations in the area.

References

Deschamps, F., S. Lebedev, T. Meier, et J. Trampert, 2008a. Azimuthal anisotropy of Rayleigh-wave phase velocities in the east-central United States, *Geophys. J. Int., 173*, 827-843, DOI:10.1111/j.1365-246X.2008.03751.x.

Deschamps, F., S. Lebedev, T. Meier, et J. Trampert, 2008b. Stratified seismic anisotropy reveals past and present deformation beneath the east-central United States, *Earth Planet. Sci. Lett., 274*, 489-498, doi:10.1016/j.epsl.2008.07.058.

Anisotropy in the Great Basin from Rayleigh Wave Phase Velocity Maps

Caroline Beghein *(University of California at Los Angeles),* **J. Arthur Snoke** *(Virginia Polytechnic Institute and State University),* **Matthew J. Fouch** *(Arizona State University)*

The Great Basin region, Nevada, is characterized by a semi-circular shear-wave splitting pattern around a weak azimuthal anisotropy zone. A variety of explanations have been proposed to explain this signal, including an upwelling, toroidal mantle flow around a slab, lithospheric drip, and a megadetachment, but no consensus has been reached.

In order to obtain better constraints on the origin of this intriguing anisotropy pattern, we performed fundamental mode Rayleigh-wave dispersion measurements using data from the USArray Transportable Array. We then inverted these measurements to obtain azimuthally anisotropic phase velocity maps at periods between 16 s and 102 s.

At periods of 16 s and 18 s, which mostly sample the crust, we found a region of low anisotropy in central Nevada coinciding with locally reduced phase velocities, and surrounded by a semi-circular pattern of fast seismic directions. Combined with recent crustal receiver function results, these short period phase velocity maps are consistent with the presence of a semi-circular anisotropy signal in the lithosphere in the vicinity of a locally thick crust. We calculated that our short period phase velocity anisotropy can only explain ~30% of the SKS splitting times, which implies that the origin of the regional shear-wave splitting signal is complex and must have both lithospheric and sublithospheric origins.

At periods between 28 and 102 s, which sample the uppermost mantle, we detected a significant reduction in isotropic phase velocities across the study region, and found more uniform fast directions with a E-W fast axis. We attributed the transition in phase velocities and anisotropy to the lithosphere-asthenosphere boundary at depths of ~60 km. We interpreted the longer periods fast seismic directions in terms of present-day asthenospheric deformation, possibly related to a combination of Juan de Fuca slab rollback and eastward-driven mantle flow from the Pacific asthenosphere.

References

Beghein, C., Snoke, J.A., and Fouch, M.J., Depth Constraints on Azimuthal Anisotropy in the Great Basin from Rayleigh Wave Phase Velocity Maps, *Earth Planet. Sci. Lett., 289*, 467-478, 2010.

Acknowledgements: This research was partially funded by NSF grants EAR-0548288 (MJF EarthScope CAREER grant).

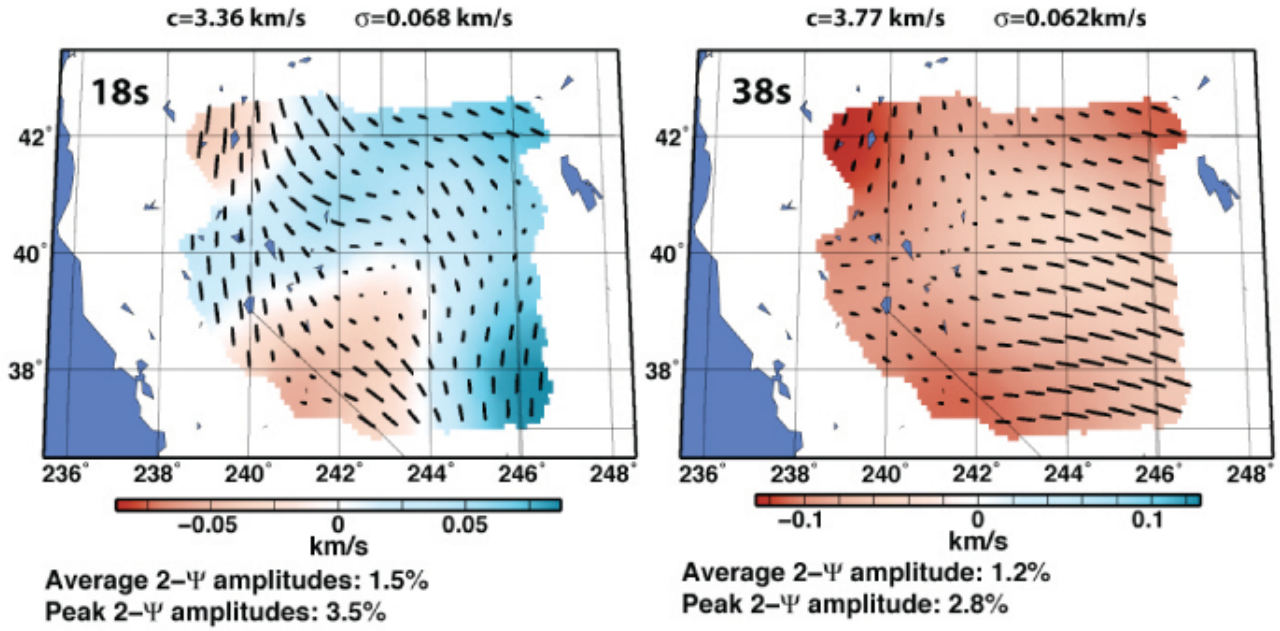

Azimuthally anisotropic phase velocity maps at 16 s and 38 s period. The background colors represent the isotropic phase velocity anomalies. The black lines show the fast direction of propagation for Rayleigh waves (2Ψ anisotropy). The reference phase velocity, calculated using the reference mTNA model defined by Beghein et al. (2010), and the average measurement uncertainty are given on top of each each map.

Source-Side Shear Wave Splitting and Upper Mantle Flow in the Romanian Carpathians and Surroundings

R. M. Russo *(University of Florida),* **V. I. Mocanu** *(University of Bucharest)*

We present shear wave splitting measurements from 5 earthquakes that occurred in the Vrancea seismic zone of the Carpathian Arc. S waves from these events, all with magnitudes > 5.4 Mw and deeper than 88 km, were recorded at broadband stations of the Global Seismic Network, and the Geoscope and Geofon Networks, and used by us to measure shear wave splitting corrected for substation splitting and anisotropy. In order to carry out these corrections we used published shear wave splitting parameters, thus isolating contributions to observed splitting from the Vrancea source region and upper mantle surrounding the Carpathian Arc. The resulting 32 good observations of source-side shear wave splitting, along with 54 null splitting observations (which yield two potential splitting directions) clearly show that upper mantle anisotropy is strongly variable in the region of the tightly curved Carpathian Arc: shear waves taking off from Vrancea along paths that sample the East and Southern Carpathians have fast anisotropy axes parallel to these ranges, whereas those leaving the source region to traverse the upper mantle beneath the Transylvanian Basin (i.e., mantle wedge side) trend NE-SW. Shear waves sampling the East European and Scythian Platforms are separable into two groups, one characterized by fast shear trends to the NE-SW, and a second, deeper group, with trends to NW-SE; also, the majority of null splits occur along paths leaving Vrancea in these NE-E azimuths. We interpret these results to indicate the presence of at least three distinct upper mantle volumes in the Carpathians region: the upper mantle beneath the Carpathian Arc is strongly anisotropic with fabrics parallel to the local arc strike; the Transylvanian Basin upper mantle fabrics trend NE-SW; and the anisotropy beneath the westernmost East European Platform may be characterized by a shallow NW-SE trending fabric concentrated in the cratonic lithosphere of the East European Platform, and a second, deeper fabric with E-W trend marking asthenospheric flow beneath the craton's base. This more complex anisotropy beneath the western edge of the East European Platform would account for both the variability of observed splitting of waves that sample this volume, and also the strong prevalence of nulls observed along eastward-departing azimuths.

References

Russo, R. M., and V. I. Mocanu, Source-Side Shear Wave Splitting and Upper Mantle Flow in the Romanian Carpathians and Surroundings, *Earth and Planet. Sci. Lett. 287*, 205-216, doi: 10.1016/j/epsl.2009.08.028, 2009.

Acknowledgements: An early version of this work was supported by National Science Foundation grant EAR-0230336.

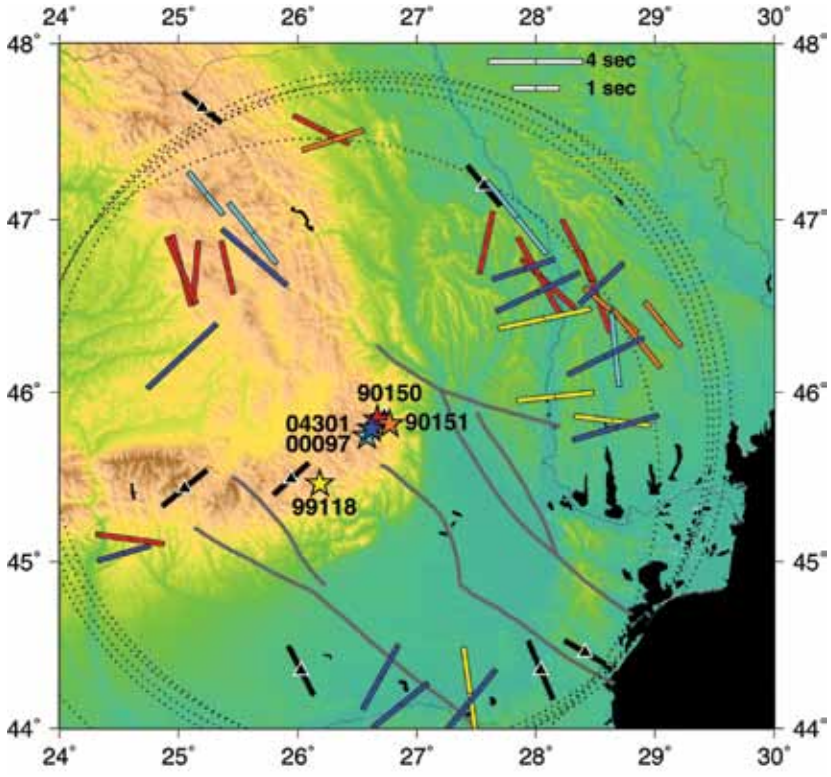

Source-side shear wave splitting results from all 5 study earthquakes, event locations (stars) and splits (bars) color coded to match. Gray circles are surface projections of 2 ÌŠ radius source lower focal hemispheres for reference. Splits plotted at surface projections of 200 km depth piercing points along event-station path to show geometry of sampling for individual event-station pairs. Splitting delay times as per key, upper right.Black bars with white bordered triangles are splitting from SK(K)S phases at stations in the study region (Ivan et al., 2008).

Source-Side Shear Wave Splitting and Upper Mantle Flow in the Chile Ridge Subduction Region

R. M. Russo *(University of Florida),* **A. Gallego** *(University of Florida),* **D. Comte** *(Universidad de Chile),* **V. I. Mocanu** *(University of Bucharest),* **R. E. Murdie** *(Goldfields Australia),* **J. C. Vandecar** *(DTM -Carnegie Institution of Washington)*

The actively spreading Chile Ridge has been subducting beneath Patagonian Chile since the Middle Miocene. After subduction, continued separation of the faster Nazca plate from the slow Antarctic plate has opened up a gapâ€"a slab windowâ€"between the subducted oceanic lithospheres beneath South America. We examined the form of the asthenospheric mantle flow in the vicinity of this slab window using S waves from six isolated, unusual 2007 earthquakes that occurred in the generally low-seismicity region just north of the ridge subduction region. The S waves from these earthquakes were recorded at distant seismic stations, but were split into fast and slow orthogonally polarized waves at upper mantle depths during their passage through the slab window and environs. We isolated the directions of fast split shear waves near the slab window by correcting for upper mantle seismic anisotropy at the distant stations. The results show that the generally trench-parallel upper mantle flow beneath the Nazca plate rotates to an ENE trend in the neighborhood of the slab gap, consistent with upper mantle flow from west to east through the slab window.

References

Russo, R. M., A. Gallego, D. Comte, V. Mocanu, R.E. Murdie, and J.C. VanDecar, Source-side shear wave splitting and upper mantle flow in the Chile Ridge subduction region, *Geology*, 38, 707-710, doi: 10.1130/GE30920.1, 2010.

Acknowledgements: This work was supported by U.S. National Science Foundation grant EAR-0126244 and CONICYT-CHILE grant 1050367.

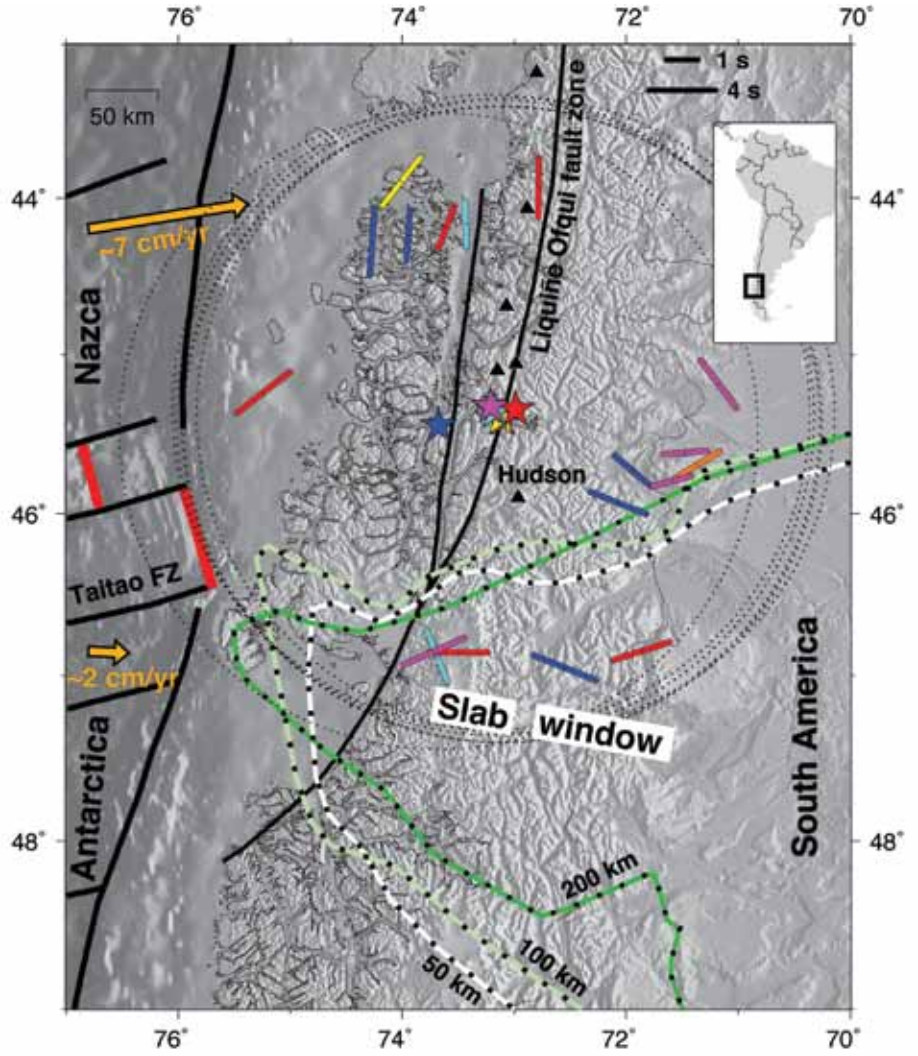

Tectonic and relief map of study region. Chile Ridge spreading centers (red) and transform-fracture zones (black) shown. Black triangles=volcanoes; FZ=fault zone. Stars mark epicenters of six study earthquakes, relocated by Russo et al. (2010) colored same as source-side splitting measurements (bars; see delay time scale, upper right). Dotted circles are 200 km radius about source events; splits plotted in azimuth of takeoff. Dashed lines mark the boundary of the slab window, defined as the "0.5% velocity perturbation con- tour at 50, 100, and 200 km depths from the tomography of VanDecar et al. (2007). Note that the northern slab window boundary is well resolved; the southern boundary is not.

An Earthscope Magnetotelluric Transect of the Southern Cascadia Subduction System, Washington

Philip E. Wannamaker *(University of Utah/EGI),* **Robert L. Evans** *(Woods Hole Oceanographic Institution)*

The first slow-slip earthquake events were observed over the Southern Cascadia Subduction system and exhibit a remarkably uniform 14 month periodicity. We collected 60 wideband magnetotelluric soundings in an east-west profile to examine state of deep crustal and upper mantle fluidization as it pertains to subduction zone locking and slow-slip nucleation. The responses of this profile are being compared to those of the earlier EMSLAB project across northwestern Oregon to the south, which is undergoing reanalysis. These results are new and not yet subject to formal non-linear inversion, but visual inspection reveals both similarities and important differences. A diagnostic high anomaly in the TM mode phase seen near the coast in Oregon is not visible in the Washington data and this tentatively is correlated with reduce fluid/subducted sediment content and greater observed plate locking for the latter area. Further inland, this phase develops more fully for both transects and is interpreted to reflect increased slab hydrate breakdown and fluid release. The inland results at lower frequencies are expected to yield geometry and physical properties of arc and back-arc melt zones of the deeper lithosphere and upper asthenosphere.

References

R. S. McGary; R.L. Evans; S. Rondenay; G. A. Abers; K. C. Creager; P. E. Wannamaker (2009), Joint magnetotelluric and seismic investigation of the Cascadia subduction zone structure: Preliminary results and outlook, EOS Trans AGU.

Acknowledgements: This project is being supported under NSF/Earthscope grants EAR08-44041 and EAR08-43725.

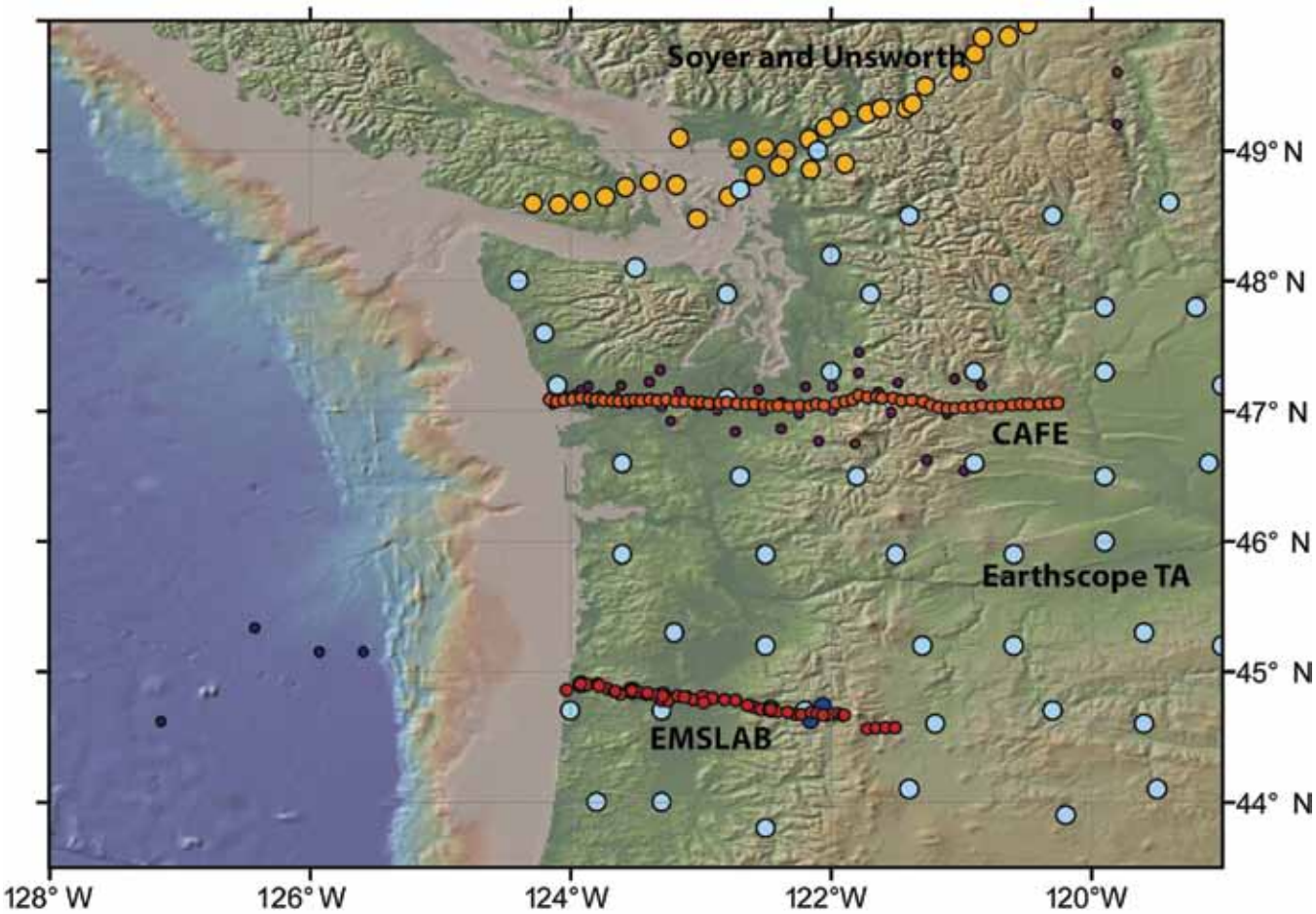

Figure 1. MT transect site distribution for the EMSLAB Lincoln Line (south) and the new Café-MT transect to the north. EMSLAB line contains 40 land sites plus seven sea-floor soundings (5 MT, 2 tipper only; see Wannamaker et al., 1989, JGR). Café line contains 60 wideband site; long-period sites are to be collected summer-fall of 2010.